

## Abstract

Non-relativistic Quantum Theory fairly accurately describes the resonance phenomena around a black hole, even though black holes are thought of as general relativistic (GR) objects. Graphically and numerically we are able to demonstrate that the form of the GR effective gravitational potential energy curves for photons and gravitons circling a non-rotating black hole which are trapped in the gravitational potential cavity surrounding a black hole, are similar to classical (non-relativistic) harmonic oscillator curves. This has been obtained for several of the lowest quantized values of graviton and photon angular momenta measured with respect to an origin situated at the center of the black hole (that is, for orbital angular momentum quantum numbers equal to  $L=2, 3, 4$  for gravitons and  $L=1, 2, 3$  for photons).

In consequence, within the equations of the Theory of General Relativity, the solutions of the lowest frequencies of photons and gravitons gravitationally trapped in orbitals while circling a black hole closely match those quantized frequencies possible for a harmonic oscillator within the non-relativistic theory of Quantum Mechanics.

These orbital frequencies are seen in the Quasi-Periodic Oscillations (QPOs) present in the Near Infrared (NIR) spectrum observed at Earth emitted from near the black hole Sgr A\* constituting the center of The Milky Way galaxy. The region of emission is closer to the black hole than the accretion disk.

Though the Theory of General Relativity is often considered incompatible with Quantum Mechanical predictions, this is an original demonstration that the General Relativistic theory, published by Einstein 9 years before Quantum Mechanics was discovered, did contain predictions matching those of non-relativistic Quantum Mechanics.



Graviton and Photon Orbitals Surrounding  
a Black Hole.  
Application to the Supermassive Black Hole at the  
Milky Way Galactic Center, With NIR  
Observational Confirmation.

Shawn Culbreth

East Carolina University Physics Department

July 19, 2013

© Shawn Culbreth, 2013

## ACKNOWLEDGEMENTS

I would like to thank my parents and family for their continued support throughout my academic career.

I would like to thank my advisor, Dr. Day, for working with me and pointing me in the right directions, for being patient with me and working hard to help me understand the equations, concepts, and ideas that led to this work.

I would like to thank Stephanie Winkler and Maneesh Jeyakumar for helping me in the research stages of this Thesis.

I would like to thank the staff and faculty of the East Carolina University Department of Physics for their help and the use of their facilities, especially Jeanne Balaoing for her help in printing materials.

I would like to thank my committee members for their help and input on my thesis.

# Contents

<b>Contents</b>	<b>i</b>
<b>List of Figures</b>	<b>iii</b>
<b>List of Tables</b>	<b>iv</b>
<b>Abbreviations</b>	<b>vi</b>
<b>1 Introduction</b>	<b>1</b>
<b>2 A Brief History of Quantum Mechanics and General Relativity</b>	<b>4</b>
2.1 Quantum Mechanics . . . . .	4
2.2 General Relativity . . . . .	5
<b>3 Black Holes</b>	<b>8</b>
3.1 Types of Black Holes . . . . .	9
3.2 How Collapse-formed Black Holes are Created . . . . .	10
<b>4 The Schwarzschild Metric</b>	<b>13</b>
<b>5 Units in General Relativity</b>	<b>15</b>
<b>6 The Resonance Cavities Around a Black Hole</b>	<b>17</b>
6.1 Using Quantum Mechanics to Approximate Resonance Phenomena . . . . .	21
6.1.1 Tortoise Coordinates . . . . .	22
6.1.2 The Harmonic Oscillator . . . . .	26
6.1.3 The Correction Terms from Perturbation Theory . . . . .	30

6.2	Properties of Trapped Photons and Gravitons . . . . .	35
6.2.1	Photons . . . . .	35
6.2.2	Gravitons . . . . .	38
6.3	How Angular Momentum Properties Influence the Orbitals . . . . .	39
6.4	Most-Stable Energy States of Trapped Photons and Gravitons within the Cavity . . . . .	43
6.5	Photon and Graviton interaction with Electrons in the Cavity Region	48
<b>7</b>	<b>Choosing a Black Hole to Observe</b>	<b>50</b>
<b>8</b>	<b>Observing the Black Hole Sgr A*</b>	<b>52</b>
8.1	NIR and X-Ray Flares . . . . .	53
8.1.1	Possible Explanations for Flares and Subflares . . . . .	54
8.2	Possible Causes of the Continuous Variability Signal . . . . .	54
8.2.1	Our Theory Explains the Continuous Variability of Sgr A* . .	55
<b>9</b>	<b>The Importance of Measuring a Graviton</b>	<b>59</b>
<b>10</b>	<b>Conclusions</b>	<b>60</b>
	<b>References</b>	<b>62</b>
	<b>Appendices</b>	<b>67</b>
<b>A</b>	<b>Additional Tables</b>	<b>67</b>

## List of Figures

1	potential squared energy curves from GR . . . . .	18
2	Potential energy curves from classical mechanics with our calculated curves from GR . . . . .	20
3	Calculated photon potentials in the tortoise coordinate system . . . .	25
4	Calculated graviton potentials in the tortoise coordinate system . . .	26
5	The harmonic oscillator curve shown with the calculated potential curve	28
6	The graphical difference of our potential from the created harmonic oscillator potential . . . . .	29
7	The effective potential energy of an L=2 graviton in r with the calcu- lated energy level . . . . .	34
8	A diagram of the shapes of P-orbitals . . . . .	41
9	A diagram of the shapes of D-orbitals . . . . .	42
10	NIR spectrum data for Sgr A* . . . . .	53
11	NIR spectrum data for Sgr A* with marked times for photon and graviton oscillations . . . . .	56



## List of Tables

1	Typically used conversion factors to unitless quantities. . . . .	16
2	Values for the harmonic oscillator potential eigenvalues for gravitons in the L=2 state. . . . .	32
3	Correction terms to the base eigenvalues for the harmonic oscillator for gravitons in the L=2 state. . . . .	32
4	Energy correction and values for different orders of perturbation theory for the L=2 state of gravitons . . . . .	33
5	Energy correction and values for different orders of perturbation theory for the L=1 state of photons . . . . .	33
6	Energy correction and values for different orders of perturbation theory for the L=2 state of photons . . . . .	34
7	The normal modes of the photon and graviton scattering potentials calculated from GR. . . . .	44
8	The normal modes of the scattering potentials calculated from GR as measured from the bottom of our potential wells. . . . .	45
9	The comparison of our calculated values and the real part of the scat- tering potential normal modes with percent error . . . . .	46
10	The number of average cycles for the lifetime of the orbitals of photons and gravitons for different values of L. . . . .	47
11	Values of $E_n^{(0)}$ for gravitons in the L=3 state. . . . .	VI
12	Values of $E_n^{(0)}$ for gravitons in the L=4 state. . . . .	VI
13	Values of $E_n^{(0)}$ for photons in the L=1 state. . . . .	VII
14	Values of $E_n^{(0)}$ for photons in the L=2 state. . . . .	VII

15	Values of $E_n^{(0)}$ for photons in the L=3 state. . . . .	VIII
16	$dV_{nm}$ terms for gravitons in the L=3 state. . . . .	VIII
17	$dV_{nm}$ terms for gravitons in the L=4 state. . . . .	VIII
18	$dV_{nm}$ terms for photons in the L=1 state. . . . .	IX
19	$dV_{nm}$ terms for photons in the L=2 state. . . . .	IX
20	$dV_{nm}$ terms for photons in the L=3 state. . . . .	IX

# Abbreviations

Abbreviation	Meaning
ELF	Extremely Low Frequency
GR	General Relativity
ISCO	Innermost Stable Circular Orbit
L	Orbital Angular Momentum
ly	Lightyear
$M_{\odot}$	Solar Masses
NIR	Near Infrared
QPO	Quasi-Periodic Oscillation
$r$	The reduced circumference in the Schwarzschild metric
$r^*$	The radius in the Tortoise Coordinate system
$s$	Spin
Sgr A*	Sagittarius A*, the Black Hole at the center of the Milky Way
V	Effective Gravitational Potential Energy

# 1 Introduction

In several ways the particles circling a black hole are similar to electrons orbiting in a hydrogen atom. The energies are quantized and the orbital shapes are of the same form; however, in place of a quantized amount of charge on the nucleus we can have a continuous value for the mass of the black hole. We can derive wave functions, for the particles around a black hole, including probability densities and lifetimes. Instead of only one type of particle circling the nucleus, we have two distinct particle types circling the black hole: photons and gravitons. In General Relativity (GR) masses curve the space-time around them. Massless particles will always follow the shortest possible path. In curved geometry, a geodesic is the shortest possible path. Massless particles will therefore follow geodesics. Since the geodesics are influenced by the curvature due to the black hole mass, the black hole has an influence on the path of massless particles and can therefore cause them to orbit the black hole.

Just as in hydrogen-like atoms (1 electron), where the energies and the wave functions can be scaled by a Z constant relating to the number of charged particles in the nucleus, we can scale the energies and wave functions by the value for the mass of the black hole; thus we obtain answers that are universally valid for any size of the mass. They can range from stellar-size, intermediate-size, to supermassive black holes centered at galactic centers. This is a range on orders of 10 to  $10^{10}$  Solar Masses [4]. The wavelengths, instead of being on the order of nano to femto-meters, range on the order of the circumference of the black holes (about  $85km$  to  $1.6 \times 10^{12}km$  - about 2 months at the speed of light). When we consider the radius of the solar system, about 5.3 hours at the speed of light [4], we can see that the wavelengths of these particles can reach 270 times the radius of our solar system. These waves can be

considered Extremely Low Frequency (ELF). ELFs generally range from 0-300  $Hz$ , making our wavelengths some of the more extreme ELFs [4].

This work constitutes an original description of the normal mode eigenstates of gravitons and photons from General Relativity (GR) as discrete energy levels in a non-relativistic quantum mechanical harmonic oscillator. The solutions to these harmonic oscillator states provide more insight into the orbital nature and energies of the normal modes. This includes the idea of standing waves existing in shaped orbitals around the outside of a black hole, near the event horizon. The graviton and photon orbitals and angular properties can be calculated through non-relativistic quantum mechanics, as if the individual particles were each the electron in a Hydrogen-like atom, due to the negligible interaction between particles. Electrons are fermions, meaning that they cannot exist in the same energy state as another electron, but this is not the case for bosons such as photons and gravitons. Bose-Einstein statistics allow for more than one boson to exist in one energy state. This, combined with the idea that the effective particle interactions are negligible compared to the interaction with the black hole, allows us to look at individual boson interactions with the black hole, as we would single electron interaction with the nucleus of an atom. Since single electrons exist in discrete energy states, we conclude similar findings for photons and gravitons. We can then apply our findings from looking at single photon and graviton interactions with the black hole, the preference for photons and gravitons to exist in specific energy states in the orbital states.

The effective potential energy in which the gravitons and photons exist in these states is a set of potential cavities around a black hole, with highest density near 1.5 times the Schwarzschild radius. These cavities exist closer than the Innermost Stable

Circular Orbit (ISCO) for particles of nonzero rest mass, meaning that they are closer to the event horizon than the accretion disk. Since the gravitational potential in GR is usually represented as a potential squared, the cavity nature of this region has yet to be studied. By taking the negative square root of the potential squared, we obtain potential energy curves that closely resemble a potential energy curve for particles in classical mechanics with non-zero orbital angular momentum. This potential consists of a potential well which allows several resonance states for the gravitons and photons. They can exist in these states with a degree of stability. The states correspond to quantum mechanical resonance states, typically seen as orbitals.

In the hydrogen atom, single electron states exist in orbitals as directed by their orbital angular momentum states. This would indicate that the gravitons and photons should also exist in orbital states due to their orbital angular momentum. The graviton and photon orbitals correspond to the same basic orbital shapes that are present in the hydrogen atom, due to the properties of the kinetic energy operator in spherically symmetric systems. This indicates that the most stable state for gravitons is a D-shaped orbital and the most stable state for photons is a P-shaped orbital.

The orbital energy of the lowest orbital can be observed in the Near Infrared (NIR) spectrum of the Supermassive Black Hole Sagittarius A\* (Sgr A\*) at the center of our galaxy. By studying the continued variability signal of Sgr A\*'s NIR spectrum, we can see the electron emissions caused by non-thermal synchrotron emission based on electron grouping due to the coherent graviton or photon interaction with electrons close to the black hole. This gives an observational confirmation of the existence of the normal mode resonances for gravitons and photons in the lowest possible orbital near the event horizon.

## 2 A Brief History of Quantum Mechanics and General Relativity

In order to fully understand the scope of this work, some background knowledge is required of the ideas behind quantum mechanics and general relativity. We provide a brief history of these two branches of physics to allow a better understanding of where the ideas, which are presented in this work, originated. We have also included background information on black holes in order to complete the basic knowledge required to better understand this work.

### 2.1 Quantum Mechanics [21]

In the early stages of optical physics, the properties of light had been explained by many different conceptual ideas, most of them being particulate in nature. The wave theory of light has been present in the scientific community since the 17th century. In 1803 Thomas Young, in his book “On the nature of light and colours,” explained the findings of his “double-slit experiment,” which proved the wave nature of light, making it the standard accepted model for the nature of light at this time.

Kirchoff, in 1859, and Boltzmann, in 1877, suggested that, in order to solve the black-body radiation problem, the energy could exist in discrete levels. It wasn't until Planck suggested that energy is radiated and absorbed in discrete amounts that people began to think of light as having a particulate form. According to Planck each energy level was directly proportional to the frequency of the light as seen in its wave nature. This was later substantiated by the photoelectric effect discovered by Einstein. These energy levels were described as “quantized” or to exist in separate

“quanta.” This is where the title of “Quantum Mechanics” comes from.

The idea that energy was quantized led to a massive influx of scientific research and ideas in the early 1900s that eventually evolved into quantum theory. Unlike classical mechanics, there is no single person that is credited with the discovery of quantum mechanics. It was instead created by dozens of scientists, such as Schrödinger, Bohr, Einstein, Planck and many others all working together. In 1927 the field of quantum physics was accepted at the Fifth Solvay Conference.

Research continued into the mid and late 1900s and there continues to be a large amount of research in this field to this day. Quantum mechanics has led to many new fields of study, such as semiconductor physics, which influence our world today. There are still many theoretical models involving basic quantum mechanical properties, such as the idea of quantum computers and quantum money (the idea that money could theoretically be coded with quantum states so that it could not be counterfeited), that are being studied to this day.

The theory of quantum mechanics is now at the core of atomic physics, physical chemistry, solid-state physics, nuclear physics and particle physics.

## **2.2 General Relativity**

In 1916, Albert Einstein developed the theory of GR in which space and time were intimately connected and that gravitational bodies warped the space-time around them [19]. This perfectly described the precession of the orbit of Mercury, which could not be explained classically. This precession, according to general relativity is caused by the slowing of time as Mercury nears the sun, due to the sun’s mass, thus causing the speed to slow near the sun and become slightly off course such



that it creates a shifted orbital path [19]. This theory was observationally proven by observing light bend around the sun; we now call this effect gravitational lensing. It enables researchers to see stars during a solar eclipse that should have been behind the sun. We now observe this phenomenon when looking at distant galaxies or clusters, and we utilize it to show where dark matter is located [13].

Another proof of general relativity was found when Pound and Rebka (1960) performed their experiment on gravitational doppler shift [30]. They used gamma rays generated by iron-57 which were then detected by exciting other iron-57 atoms above or below the position of the source. This meant that the light frequency needed to remain constant in order for the photon to be absorbed. At first there was no absorbance, indicating that the light frequency was gravitationally shifted. In order to find the exact shift, Pound and Rebka put the source in motion in order to obtain a special relativistic doppler shift which cancelled the gravitational shift. This allowed the iron-57 atoms to absorb the frequency. Their results found that the general relativistic equations to determine gravitational frequency shift were validated by their experiment.

More recently, the Nobel Prize in 1993 was awarded to Hulse and Taylor for the use of their discovered binary pulsar system to study the loss in angular momentum of the system and provide indirect evidence of the existence of gravitational waves, as predicted by general relativity [12]. Much like it is understood that light is composed of photons, it is believed that these gravitational waves are composed of gravitons. This thesis focuses on the idea of having trapped gravitons in a gravitational potential cavity around a black hole. The gravitational potential cavity exists due to the curvature of space-time caused by the black hole mass. Gravitons become temporarily

trapped in the cavity. Photons can also become temporarily trapped in a cavity around the black hole, in a similar manner to the gravitons. The properties of these trapped photons and gravitons will be discussed further in section 6.2. The specific angular momentum properties will be discussed in section 6.3.

### 3 Black Holes

General relativity also predicted that there could be an object so dense that not even light could escape its gravitational pull. Since the theory states that light moves at the maximum speed, nothing could escape the dense object. This is due to the idea that time as seen by a far away observer stops at the point which light can no longer escape. The radius at which this happens is known as the event horizon. Wheeler named this object a black hole based on the idea that it would be completely black since it will not emit light [36]. The black hole was thought to be purely theoretical until it was discovered in 1957 and then found at the center of nearly every galaxy we know of, with the exception of some irregular galaxies, in the 1990s [4].

In short, a black hole is a gravitational singularity. This indicates that a black hole has an infinite density at its center but it does not mean that a black hole has infinite mass; rather, it indicates that the mass of the black hole is present in an infinitely small space as seen by an outside observer [4]. Since the mass is concentrated at the center of an infinitely small point, making the radius of the mass negligible, the black hole is characterized by its event horizon. The event horizon is dependent on the mass and spin of the black hole; so, it is used as a property to see how black holes differ from one another.

As the precursor to a black hole collapses, angular momentum conservation causes it to spin faster and causes the material around it to flatten and form a disk. As material falls into the black hole, an accretion disk is formed similar to the rings of the four gas planets in our own solar system. The inner part of this disk is the innermost stable circular orbit (ISCO). The inner part of the accretion disk is considered to begin at the ISCO, which will be discussed further in section 3.1. Any orbiting particle of

nonzero rest mass within the ISCO falls inward rapidly toward the black hole. This disk is made up of elementary particles, gas, dust, rocks, stars and any other objects that the black hole can cause to orbit it, but all objects are torn apart before reaching the black hole [36].

### 3.1 Types of Black Holes [4]

There are three basic size distinctions for black holes: stellar-mass, intermediate-mass, and supermassive.

Stellar-mass black holes are the most common, and they have a mass range of 3-15 solar masses ( $M_{\odot}$ ). These black holes are the result of a core collapse of a supergiant star. They can also be formed if a neutron star, a core collapse remnant, is in close enough binary orbit that it strips mass from a secondary object until the pressure on neutrons exceeds the degeneracy pressure (due to the exclusion principle of fermions) causing the neutron star to collapse into a black hole.

Intermediate-mass black holes exist in the mass range of about 100-1000  $M_{\odot}$  but have only been shown to exist by ultraluminous X-ray sources. They seem to exist only in the center of globular clusters and very small galaxies. This suggests the possibility that they may be correlated with the creation of globular clusters, but no one is certain how intermediate-mass black holes are formed.

Supermassive black holes have been found to exist in the center of galaxies, such as our own. These have masses on the order of  $10^5$ - $10^9$   $M_{\odot}$ . The black hole at the center of our galaxy, named Sgr A\*, has a mass of about  $3.7 \times 10^6$   $M_{\odot}$ . It is believed that these supermassive black holes aid in the creation and stability of a galaxy, but that has not been confirmed. What is known is that Quasi-Stellar Objects (QSOs,

also known previously as Quasi-Stellar Radio-sources, QSRs or Quasars) are black holes which are actively accreting in the center of premature galaxies. This indicates that supermassive black holes actively accrete mass as galaxies form. They also accrete mass when galaxies collide and introduce an instability into the galaxies. The brightest supermassive black hole that we know of, the one in the center of the galaxy M87, can absorb up to  $3M_{\odot}$  worth of material per year. At about  $6 \times 10^9 M_{\odot}$  at a distance of  $6.3 \times 10^7$  lightyears (*ly*), M87 contains the largest black hole in our local universe. There are about 40 galaxies in the Local Group, the galaxy cluster containing the Milky Way, which is right beside a cluster of about 1500 large galaxies known as the Virgo Cluster. M87 is the central galaxy of the Virgo Cluster, making it an important and incredibly large galaxy that is relatively close to our own, compared to any other galaxy of its size. M87 will be discussed in section 7, when we discuss choosing a black hole for observation.

Primordial black holes are believed to have existed during the early stages of the universe. They ranged in size from about  $10^{-8}kg$  to  $10^5 M_{\odot}$ . As of yet, there is no experimental evidence to support the existence of primordial black holes.

### **3.2 How Collapse-formed Black Holes are Created**

The model generally used of black hole creation is through massive object collapse. This is because it is the only form of black hole creation that we have been able to observe. The collapse method of creation is how stellar mass black holes are formed. It has been applied, in theory, to the formation of other types of black holes, such as supermassive black holes, but there are many competing theories for how these larger black holes are formed [4].

The collapse-form model starts with a massive star, with mass at least  $20 M_{\odot}$ . A massive star, like our sun, fuses hydrogen in its core [33]. As it ages it loses hydrogen in the core and gravitationally shrinks until it has enough energy to fuse helium. The star then swells due to the energy production from the helium fusion. This continues for higher and higher elements until iron is reached. Iron has the highest nuclear binding energy, which means the fusion of iron results in a net energy loss. When the star would fuse iron in its core, it instead continues to fuse lower order elements around the core, but nothing inside the core. As the iron builds in the core, the energy from the fusion reaction keeping the star bloated begins to fail. This causes the star to collapse gravitationally and, due to angular momentum conservation, to spin rapidly [4].

What results from this collapse is entirely dependent on the mass of the collapsing star. If the star is large enough the heat produced from the collapse will cause protons and electrons to combine into neutrons. Since these neutrons are uncharged, they are able to form a very dense object at the center of the collapse. The neutrons are held apart from one another by degeneracy pressure [4]. The degeneracy pressure is due to the fact that fermions cannot exist in the same state, so as the neutrons occupy the space of nearby neutrons, the Pauli exclusion principle causes their momentum to differ more intensely. Higher momentum states are occupied based on this forced difference, which exerts a pressure [4]. A core remnant formed by neutrons held into a sphere by degeneracy pressure is called a neutron star, but if the star is large enough the degeneracy pressure will be overcome and the object will collapse further into a black hole. The black hole will form if the density of any part of the core remnant is high enough such that that mass is contained within the Schwarzschild radius.

The outer layers of the star are often expelled from molecules bouncing off the core remnant resulting in a supernova explosion. Sometimes, when a black hole is formed, instead of the matter exploding outward, the matter continues to fall into the singularity and adds to the mass of the black hole[33].

## 4 The Schwarzschild Metric

A metric is a way to measure from one point to another in curved space-time. The Schwarzschild metric uses a measurement system of a non-spinning, spherical geometry and gives a way to measure the distance from the black hole dictated by the reduced circumference and time as measured from far away [38]. The reduced circumference gives a radius as measured by taking the circumference divided by  $2\pi$ . The reduced circumference is used since there is no technical way to measure a black hole's radius from the center. The Schwarzschild metric, which makes the assumptions that the object is spherical, uncharged, not spinning, and exists in a vacuum is commonly used as the simplest approximation of massive objects such as stars or black holes [38]. To simplify a black hole system, we use the Schwarzschild metric as our reference. A black hole that is spherical, uncharged, and not spinning has yet to be found, so the Schwarzschild metric is strictly an approximation.

The thought experiment commonly used to explain the use of the reduced circumference is that someone is trying to measure the radius of the black hole using rods of material that are all the same length. As the rods approach the black hole they start to decrease in length to an outside observer even though they remain constant to the people in the frame of the rod. This is due to the bent space in which the rods exist. It means that there is no way to accurately measure the radius as seen by an outside observer by simply measuring straight from the center. Instead, the radius must be measured by the circumference since that is located at the same distance from the black hole at all times by definition. Measuring the circumference ensures that gravitational length shifting effects will not influence the distance measurement around the black hole; therefore, it gives a reasonable understanding of a locational



radius.

To find the event horizon in the Schwarzschild metric (also known as the Schwarzschild radius), we use a classical mechanical approach by finding the escape velocity. We set it to the speed of light ( $c$ ) and solve for  $R$ . This gives  $R = 2GM/c^2$ . By using the convention of removing the fundamental constants we get that  $R = 2M$ . Since we also typically remove the mass dependence, the radius of the event horizon is at a unitless position of 2 away from the black hole. Note that the event horizon is not a physical point, but rather a mathematical location at which light can no longer escape. It is used as the radius of the black hole but there is no physical surface there. It is important to note that in the Schwarzschild metric, the only criterion to have a black hole is that the entire mass of the object be contained within the Schwarzschild radius. The aforementioned ISCO is the closest point at which material can maintain a completely stable orbit and exists at the point  $r = 6$  in the Schwarzschild metric.

This unitless conversion is commonly used in the study of black holes. This is due to the idea that all black holes in the Schwarzschild metric are the same except for their masses, which makes the equations valid for all black holes. This means that length normally in meters can be expressed as a unitless quantity based on mass, which is how we scale our equations for different black holes. This will be referred to at greater length in section 5.

## 5 Units in General Relativity

In most areas of physics it often becomes useful to express terms in units other than typical SI units. In general relativity, however, it is often that the units used are typically unconventional or manipulated such that the quantities become unitless and therefore allow them to be applied universally.

For example, angular momentum which usually has units of  $Js$  can be divided by  $G/c$ , where  $G$  is the gravitational constant and  $c$  is the speed of light, to give units of  $kg^2$ . The unit is then dependent on the mass of the black hole, meaning that we can divide the momentum by  $M^2$ , where  $M$  is the mass of the black hole, to get a unitless quantity for the angular momentum.

In general relativity, this same kind of unit conversion is applied to nearly all quantities to make them unitless and therefore easier to work with, as well as valid for all acceptable values of  $M$ .

In addition to making unitless quantities, sometimes it makes more sense to express units of mass as length, or time, time as mass, or length or length as time or mass. This is usually used to express qualities of large objects. For example, the Sun has a mass of  $1.99 \times 10^{30}kg$  which can be converted to about  $1.477km$  by multiplying the mass of the sun by  $G/c^2$ . This indicates that if the mass of the sun were contained in a  $2.954km$  radius (the Schwarzschild radius,  $r=2$ ), it would be a black hole.

The common conversion units, to pure numbers, for certain quantities are shown in Table 1. We will use dimensionless quantities throughout most of this paper. If no units are presented, the quantities are dimensionless.

Quantity	Normal Unit	Unitless Conversion Factor
Distance	$m$	$\frac{GM}{c^2}$
Time	$s$	$\frac{GM}{c^3}$
Angular Momentum	$J s$	$\frac{G}{M^2 c}$
Energy	$J$	$M c^2$

Table 1: The typical unit conversions for distance, time, energy, and angular momentum units to unitless quantities. This is commonly used in GR to represent these quantities as mass scaled pure numbers to apply them to all black holes.

## 6 The Resonance Cavities Around a Black Hole

Classically, as an object approaches an object such as a black hole, the gravitational potential drops continuously to negative infinity. This is not the case in general relativity. Typically the potential is represented as the potential squared given by Equation 6.1. This was first derived by Regge and Wheeler in 1957. Chapter 4 of Chandrasekhar's book entitled *The Mathematical Theory of Black Holes* from 1992 contains an explanation of these potential squared curves[5] (see also Taylor and Wheeler's book entitled *Exploring Black Holes* from 2000 [36]). The  $V$  in the equations represents the gravitational effective potential energy. The  $s$  represents the spin of the particle,  $L$  represents the orbital angular momentum, and  $r$  represents the reduced circumference. This equation is valid in the Schwarzschild metric.

$$V^2 = \left(1 - \frac{2}{r}\right) \left(\frac{L(L+1)}{r^2} + \frac{2(1-s^2)}{r^3}\right) \quad (6.1)$$

Equation 6.1 is represented graphically in Figure 1, but for the purpose of this work, we will look at the potential provided by the negative square root of the potential squared, as seen in Equation 6.2.

$$V_{L,s} = -\sqrt{1 - \frac{2}{r}} \sqrt{\frac{L(L+1)}{r^2} + \frac{2(1-s^2)}{r^3}} \quad (6.2)$$

Equation 6.1 looks like a scattering potential due to the "hump" shape. Equation 6.2 takes the effective potential with a "hump" and turns it into an effective potential well. The negative square root is taken (rather than the positive) in order to behave as the classical gravitational potential. Given the idea that, as seen from far away, time stops as particles approach the event horizon, the potential energy should go to

zero at  $r = 2$ , and not exist for  $r$  less than 2. If we look at Equation 6.2, we see that the  $\sqrt{1 - \frac{2}{r}}$  factor goes to zero at  $r = 2$  and is imaginary beyond that point.

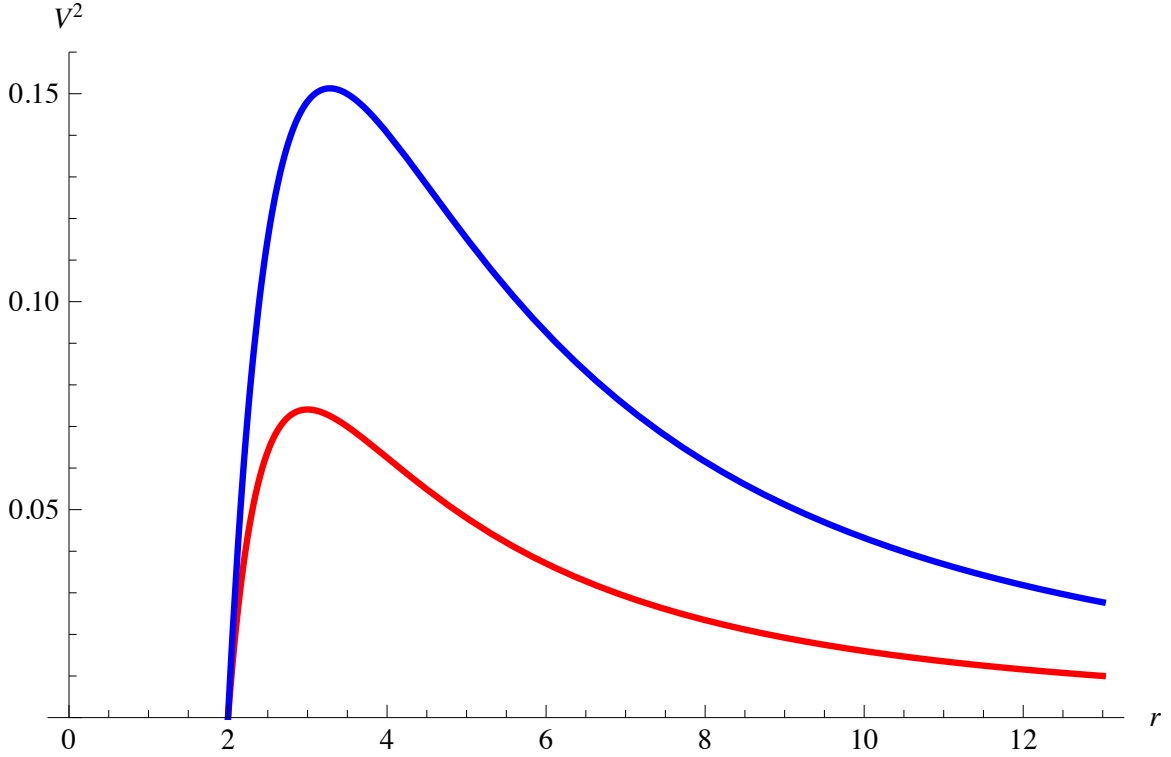


Figure 1: The potential squared is the typical representation of the potential energy in GR. This is due to the dependence on the energy squared in GR equations. The Red curve represents the potential squared for photons, while the Blue curve represents the potential squared for gravitons. As was discussed in section 4, all quantities shown are dimensionless.

The classical curve for a gravitational potential as well as the negative gravitational potentials from general relativity are seen in Figure 2 to provide a graphical representation of the effective potential energy curves. Both the photon and graviton curves are represented for their lowest lying energy states ( $L=1$  for photons and  $L=2$  for gravitons).

For particles attracted to a central object of mass  $M$ , classically the gravitational

potential energy is  $\frac{-GM}{r}$ . Since  $r$  is already scaled by  $GM$  in our units, the classical potential is seen as  $-\frac{1}{r}$  for large  $r$ . For a standing wave in spherical coordinates, the GR effective potential energy includes a component based on  $\sqrt{L(L+1)}$ , shifting the limit for  $r$  large to a lower value, introducing properties of the circling particle into the GR effective potential energy, as well as the mass of the central object.

The classical equations do contain a term due to the angular momentum of circling particles, which have a  $1/r^2$  dependence. The GR potentials always go to zero at the event horizon ( $r = 2$ ) due to time dilation as seen from afar [36].

Photons and gravitons of certain frequencies exist in standing waves as they circle the black hole. This will be further expanded upon in section 6.2.

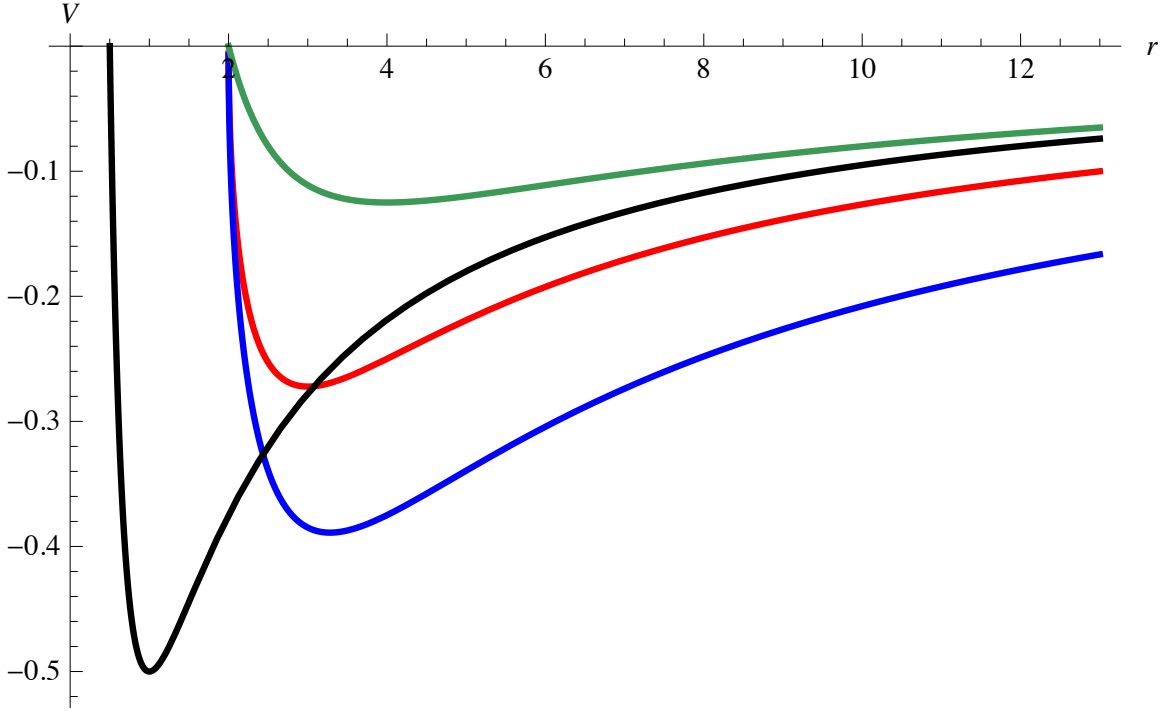


Figure 2: The potential energy curve from classical  $V = -\frac{1}{r} + \frac{L^2}{2r^2}$  is depicted in Black (L=1) and Green for L=2. These are the classical gravitational potential energy curves for particles with non-zero rest mass and non-zero angular momentum. We did not include the classical curves for L=0 since no particle we worked with can exist in an L=0 state. In Red is the gravitational potential curve for a photon with  $s=1$  and least allowed orbital angular momentum, L=1, and in Blue is the Graviton gravitational potential curve for  $s=2$  with least allowed orbital angular momentum, L=2. Both the Photon and Graviton curves are given by the equations above.

The photon effective potential energy well (Equation 6.2) has lowest position at  $r = 3.000$ . The graviton effective potential energy well has a minimum at  $r = 3.281$ . This indicates that the lowest lying states for photons and gravitons should exist near these radii.

Since these cavities exist within the ISCO, we do not anticipate that they contain completely stable orbits. Instead, we anticipate what is known as a “leaky cavity.” A leaky cavity is a cavity containing particles with a real and imaginary part to

their energies and therefore frequencies, indicating that they have a half-life within the cavity. This half-life means that the particles will eventually leave the cavity by falling into the black hole or moving to a far distance from the black hole. In order for the cavity to maintain a population of particles, the cavity acquires new particles to replace the ones that are lost.

There exists a net attractive force, or inclusion principle, between large groups of bosons and individual bosons that causes the individuals of proper frequency to enter the same phase and direction as the group, as explained by Kaniadakis and Quarati [23]. This net attractive force is what causes the photons and gravitons of correct frequency from outside the cavity to enter coherently into the resonance state within the cavity, thus replacing those that were lost due to the leaky nature of the cavity .

## **6.1 Using Quantum Mechanics to Approximate Resonance Phenomena**

The effective potential energy within the cavities looks like a harmonic oscillator potential near the bottom of the curve. The harmonic oscillator potential is the most common potential found naturally and its eigenvalues and eigenfunctions can be solved using the methods found in quantum mechanics.

In quantum mechanics, a resonance state is simply classified as the preference for a particle to exist in one state over another. Since photons and gravitons are uncharged bosons, large numbers of them can exist in the same state and they negligibly interact, unlike electrons which obey Fermi statistics and contain repulsive charge. This means that not only can photons and gravitons exist in the same state, but the only significant interaction in the system is between the individual photons



or gravitons and the black hole. This means that each photon or graviton can be treated separately when calculating the eigenfunctions (or “orbitals”) occupied by individual bosons. There is a quantum effect known as the inclusion principle that causes bosons of the same frequency to experience a net force towards coherence [23] as was mentioned earlier, in section 6. This forces the photons and gravitons in the resonance states to be coherent with one another and thus occupy the same orbital. This interaction does not effect the energy of the bosons since they must already be of the same frequency, so the energy calculations for trapped photons and gravitons inside the cavity will not be effected by this interaction.

To compare the gravitational effective potential to a harmonic oscillator, it is convenient to change coordinate systems so that this potential mirrors even better the harmonic oscillator potential by removing the sharp rise to zero on the left hand side of the potential. We do this by using what is known as the “tortoise coordinate” system.

### **6.1.1 Tortoise Coordinates**

The tortoise coordinate system is used to alleviate issues caused by singularities or discontinuities in a function, like we have at the event horizon. The name ”tortoise coordinate” is an allusion to the story from Zeno’s Paradox of the Tortoise and Achilles. The story goes that the tortoise challenges Achilles to a race so long as the tortoise receives a head start. After Achilles agrees, the tortoise tells Achilles that he will never be able to reach him since Achilles must first cover the distance already traveled by the tortoise. In this time the tortoise will have traveled a distance, however small, that Achilles must then also make up. This means that Achilles would

never be able to reach the tortoise to overtake him [31].

The story gives an explanation of what the tortoise coordinate system does. It makes it such that we are able to approach the event horizon as  $r \rightarrow -\infty$  but we are never able to reach it. This effectively removes the complications brought upon by the event horizon from our calculations by eliminating the sharp rise of the potential energy near  $r = 2$ . The system accomplishes this by the use of the natural log function, which approaches negative infinity as the argument approaches zero. The conversion equation between  $r$  and  $r^*$  (the radius in tortoise coordinate)[5] is given by:

$$r^* = r + 2 \ln\left(\frac{r}{2} - 1\right) + C \quad (6.3)$$

where  $C$  is a constant used to shift the conversion to any numerical or graphical location that is desired as part of the conversion.

In order to put the effective potential into tortoise coordinates, we needed to solve the conversion equation for  $r$  in terms of  $r^*$  and input it into the potential equation. The conversion equation can only be solved numerically by the use of the ProductLog function since it is not analytical. The ProductLog function is a representation of the numerical solution to the equation  $y = x + \ln(x)$ . The solution to the coordinate conversion is then given by:

$$r = 2(1 + \text{ProductLog}(\sqrt{e^{-2-C+r^*}})) \quad (6.4)$$

Substitution into the effective potential energy equation (6.2) gives us an effective potential energy equation in the Tortoise Coordinate system (Equation 6.5). We

center the function at zero to facilitate calculations. Setting the derivative of the potential equation to zero at  $r^* = 0$  determines the value of  $C$  to center the effective potential at  $r^* = 0$ . We found this value to be -1.615 for all  $L$  values of photons. Since the graviton curves were not all centered at the same radius, the different momentum levels for gravitons had different constants.  $C = -2.514$  for the  $L = 2$  state, -2.000 for the  $L = 3$  state, and -1.955 for the  $L = 4$  state. The equation for the effective gravitational potential energy curves is:

$$V_{L,s}(r^*) = -\sqrt{1 - \frac{2}{2(1 + \text{ProductLog}[\sqrt{e^{-2-C+r^*}}])}} \quad (6.5)$$

$$\times \sqrt{\frac{L(L+1)}{(2(1 + \text{ProductLog}(\sqrt{e^{-2-C+r^*}})))^2} + \frac{2(1-s^2)}{(2(1 + \text{ProductLog}[\sqrt{e^{-2-C+r^*}}])^3}}$$

$V_{L,s}(r^*)$  effective potentials, for both photons and gravitons ( $s=1$  and  $s=2$ ), for the three lowest angular momentum states, are graphically represented in Figures 3 and 4.

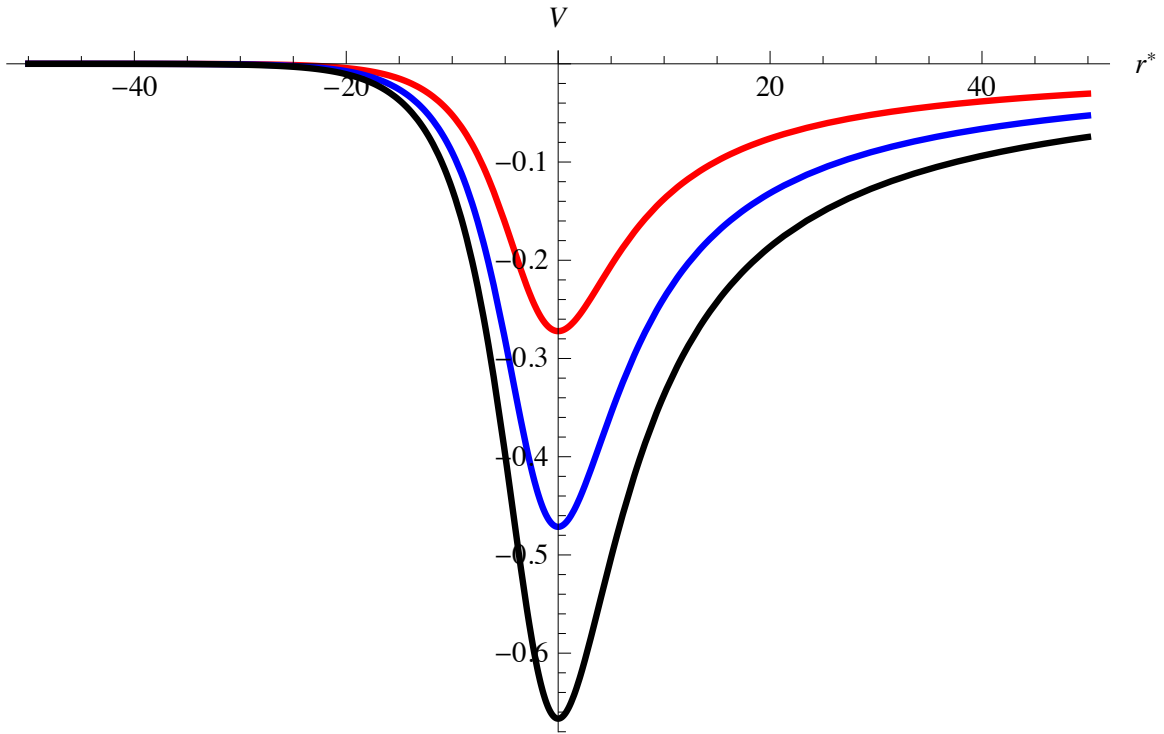


Figure 3: This shows the three different calculated photon potentials in the tortoise coordinate system. The Red curve shows the potential well for  $L=1$  photons. This is the most preferred state for photons, despite not being the deepest well, because it has the longest lifetime. The Blue curve shows the potential well for  $L=2$  photons and the Black curve shows the potential well for  $L=3$  photons.

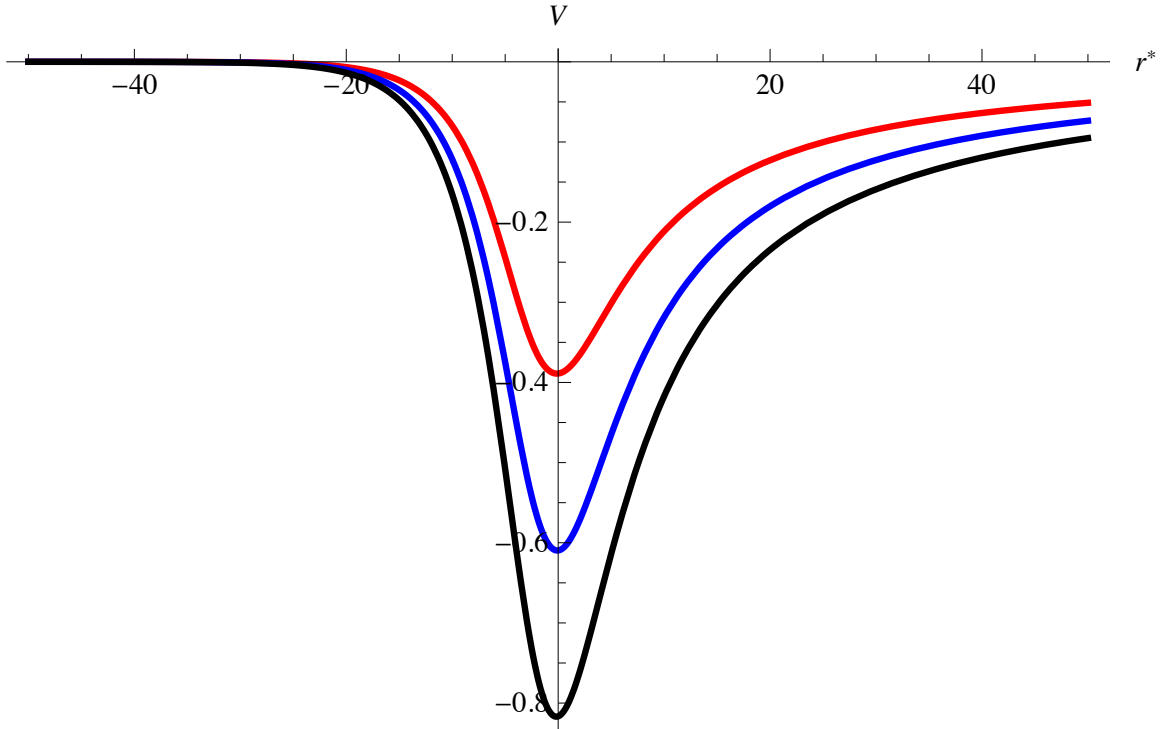


Figure 4: This shows the three different calculated graviton potentials in the tortoise coordinate system. The Red curve shows the potential well for  $L=2$  gravitons. This is the most preferred state for gravitons, despite not being the deepest well but with the longest lifetime. The Blue curve shows the potential well for  $L=3$  gravitons and the Black curve shows the potential well for  $L=4$  gravitons. Note that the potential well is deeper for the preferred state of gravitons than it is for the photon preferred state, but the states with the same orbital angular momentum are deeper for photons than for gravitons.

### 6.1.2 The Harmonic Oscillator

Harmonic oscillators are expressed by Equation 6.6, so, in order to match it, we needed to find the proper value of  $k$  to fit our curve. Since  $k$  is based on the curvature of the function, the numerical value of the second derivative of the potential at  $r^* = 0$  will provide the appropriate  $k$  value.

$$\ddot{r}^*|_{r^*=0} = k \quad (6.6)$$

$$V = \frac{1}{2}k(r^*)^2 \quad (6.7)$$

Calculating the  $k$  value from Equation 6.6 allowed us to generate a harmonic oscillator potential energy (Equation 6.7) that fits our potential, as seen in Figure 5. We also calculated the primary wave function for the harmonic oscillator (Equation 6.8).

$$\psi = \frac{\left(\frac{k}{2}\right)^{1/4}}{\sqrt{\pi}} \times e^{-\left(\frac{k}{2}\right)^{1/2}(r^*)^2} \quad (6.8)$$

This showed that the two functions were in basic agreement in the area contained by the wave function. Figure 6 shows the difference between the harmonic oscillator function and our potential to show more clearly how the two compare within the area contained by the wave function, given by Equation 6.8.

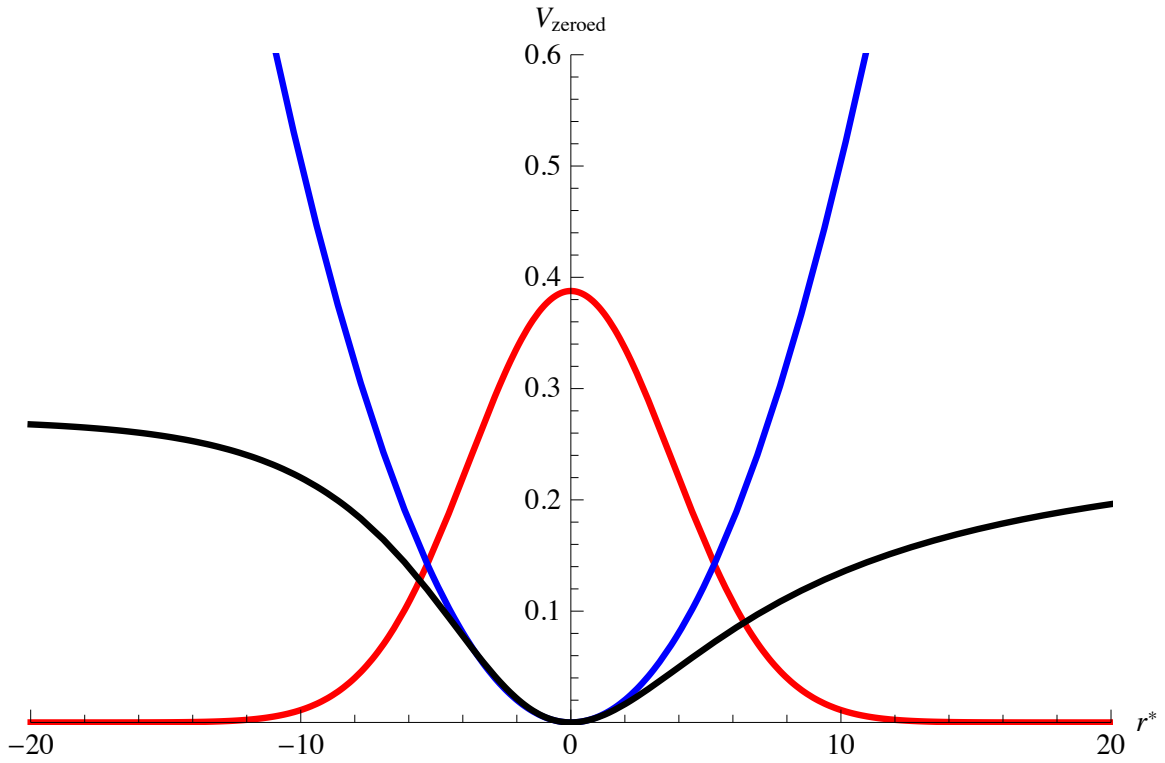


Figure 5: The generated harmonic oscillator function (given by Equation 6.7) for the  $L = 1$  photon state is shown in Blue on the same graph as the  $L=1$  state for photons, in Black, to show the fit. The photon curve has the lowest point of the potential placed at zero in order to shift the potential upward by a constant such that it is always positive. The first order wave function (given by Equation 6.8) is shown in Red to highlight the important regions of the fit.

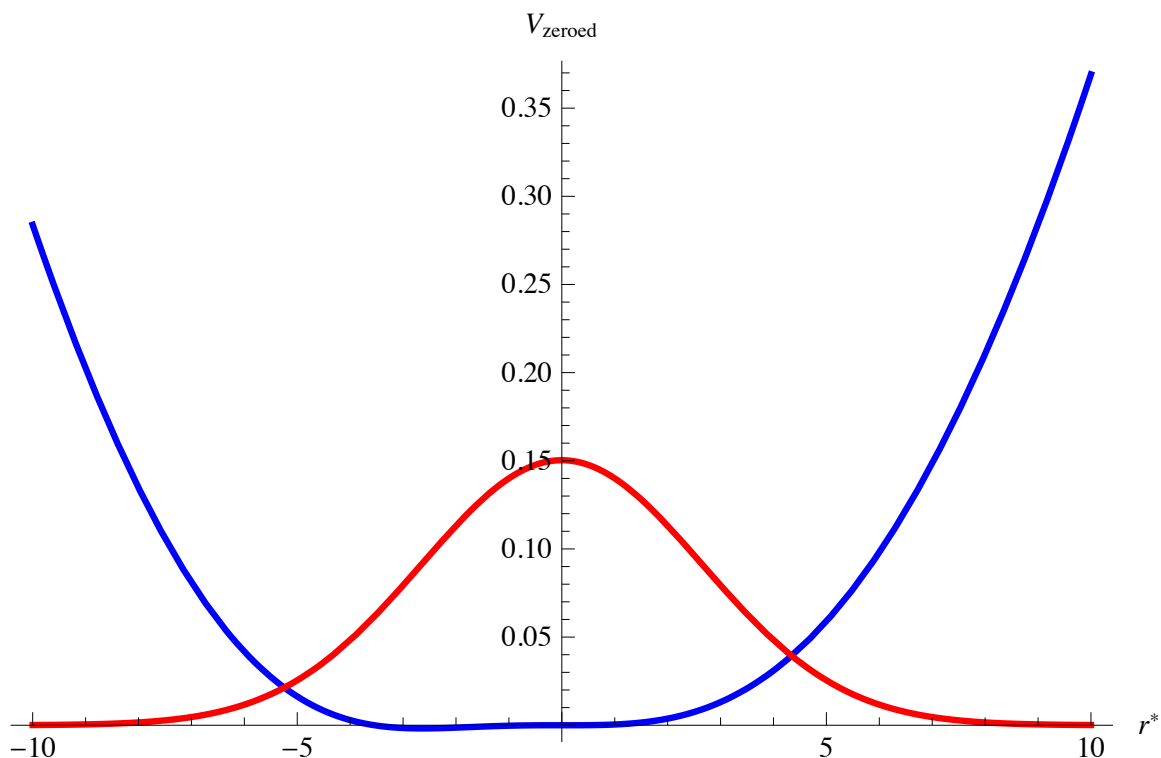


Figure 6: The Blue curve shows the potential energy difference between the photon gravitational potential energy for  $L=1$  and the harmonic oscillator potential with the same curvature. This shows how well the two curves fit within the regime covered by the wave function, in Red.

Figure 6 shows that the harmonic oscillator potential is a decent approximation for the potential curve in the regime where the wavefunction is non-zero.

We calculated the eigenvalues for the harmonic oscillator curve,  $(n + \frac{1}{2})\hbar\omega_0$  with  $\hbar = 1$ ,  $\omega_0 = \sqrt{\frac{k}{m}} = \sqrt{2k}$ , and  $n=0, 1, 2, \dots$  in our units. The eigenvalues for the harmonic oscillator are presented in Table 2 on page 32. We then used correction terms from perturbation theory to correct these eigenvalues so that they fit our potential more closely.

The wave function in Figure 5 shows how the wave function fits into the potential



well. The wave function does exist outside of the potential but with positive curvature, as is common in harmonic oscillator wave functions. The probability density (the square of the wave function) falls as the wave function becomes farther from the potential, but does provide a probability for the particle to exist outside of the potential. This tells where the primary shape of the orbital exists. For photons this shape is a "teardrop," as seen in Figure 8 on page 41, with the lowest probability closer to the black hole. The orbital shape will be discussed in further detail in Section 6.3.

### 6.1.3 The Correction Terms from Perturbation Theory

Perturbation theory is often used in quantum mechanics as a tool to more accurately describe a complex system. The general idea behind it is to take a system that is known and matches fairly well, such as the harmonic oscillator potential, and continually correct the eigenvalues and eigenfunctions toward those of the more complex potential. It does not usually take many correction terms to obtain accurate values, if the two potentials are quite similar as in our case.

The harmonic oscillator energy eigenvalues were corrected in the form of Equation 6.9, using Equations 6.13 - 6.17, from perturbation theory, with definition of terms given by 6.10 - 6.12. The numerical values for the  $dV_{nm}$  and  $E_n^{(0)}$  terms, given by Equations 6.12 and 6.13 respectively, are shown in Tables 2 and 3 for gravitons in the L=2 state.

$$E_n = E_n^{(0)} + E_n^{(1)} + E_n^{(2)} + E_n^{(3)} + E_n^{(4)} + \dots \quad (6.9)$$

$$E_{nm} = E_n^{(0)} - E_m^{(0)} \quad (6.10)$$

$$dV = V_{GR} - \frac{1}{2}kr^{*2} \quad (6.11)$$

$$dV_{nm} = \langle n^{(0)} | dV | m^{(0)} \rangle \quad (6.12)$$

$$E_n^{(0)} = \langle n | \frac{1}{2}kr^{*2} | n \rangle \quad (6.13)$$

$$E_n^{(1)} = dV_{nn} \quad (6.14)$$

$$E_n^{(2)} = \sum_{k_2} \frac{|dV_{nk_2}|^2}{E_{nk_2}} \quad (6.15)$$

$$E_n^{(3)} = \sum_{k_3, k_2} \frac{dV_{nk_3} dV_{k_2 k_3} dV_{k_2 n}}{E_{nk_2} E_{nk_3}} - dV_{nn} \sum_{k_3} \frac{dV_{nk_3}}{E_{nk_3}^2} \quad (6.16)$$

$$E_n^{(4)} = \sum_{k_4, k_3, k_2} \frac{dV_{nk_4} dV_{k_4 k_3} dV_{k_3 k_2} dV_{k_2 n}}{E_{nk_2} E_{nk_3} E_{nk_4}} - E_n^{(2)} \sum_{k_4} \frac{|dV_{nk_4}|^2}{E_{nk_4}^2} \quad (6.17)$$

$$- 2dV_{nn} \sum_{k_4, k_3, k_2} \frac{dV_{nk_4} dV_{k_3 k_4} dV_{k_2 n}}{E_{nk_3}^2 E_{nk_4}} + dV_{nn}^2 \sum_{k_4} \frac{|dV_{nk_4}|^2}{E_{nk_4}^3}$$

We calculated the perturbation corrections to the third order to find results that closely match those from GR scattering calculations (which will be discussed in section 6.4). Tables 4, 5, and 6 show our calculated correction terms to the energy as well as the energy values after the correction for that order. We did not calculate higher orders due to the complexity of the fourth order correction in perturbation theory. The location of this energy level is placed on the potential energy curve for the L=2 state for gravitons in Figure 7 to give a graphical representation of where this energy level is at. It is important to note that the calculated values are read from the bottom of the curve, while the actual energy, which is used to calculate the frequency,

is measured from the zero point on the energy. This means that the actual energy value for our oscillations is the calculated value minus the value at the bottom of the curve.

Harmonic Oscillator Eigenvalue	Numerical Calculation
$E_0^{(0)}$	0.0392
$E_1^{(0)}$	0.118
$E_2^{(0)}$	0.196
$E_3^{(0)}$	0.275
$E_4^{(0)}$	0.353
$E_5^{(0)}$	0.432
$E_6^{(0)}$	0.510

Table 2:  $E_n^{(0)}$  terms, in a basis of two harmonic oscillator wave functions for gravitons in the state L=2. These correction terms are used in the perturbation theory corrections.

Wave Function	$ U_0 \rangle$	$ U_1 \rangle$	$ U_2 \rangle$	$ U_3 \rangle$	$ U_4 \rangle$	$ U_5 \rangle$	$ U_6 \rangle$
$\langle U_0  $	-0.00421	-0.0289	-0.0169	.000893	-0.00892	.000764	.00268
$\langle U_1  $	-.0288	-0.0281	-0.0393	-.0471	.00349	-.0134	.000410
$\langle U_2  $	-.0168	-0.0393	-0.0738	-.0480	-.0815	.00569	-.0167
$\langle U_3  $	.000893	-.0471	-.0480	-.129	.0461	.117	.00760
$\langle U_4  $	-0.00892	.00349	-.0815	.0461	.191	-.0471	-.156
$\langle U_5  $	.000764	-.0134	.00569	.117	-.0471	-.256	-.0475
$\langle U_6  $	.00268	.000410	-.0167	.00760	-.156	-.0475	-.323

Table 3:  $dV_{nm}$  terms for perturbation theory for various combinations of wave functions and  $dV$ , given by Equation 6.12 for gravitons in the L=2 state. The table is arranged such that the Bra and Ket are each with  $dV$ , producing the value for  $dV_{nm}$  at the location of the intersection on the table of the Bra and Ket. The intersection values represent the value of  $dV_{nm}$  where  $n$  is the wavefunction on the left and  $m$  is the wavefunction on the right. This is presented for a basis of seven wave functions

Perturbation Order	Perturbation Value	Energy After Inclusion
$E_0^{(0)}$	.03927	.03927
$E_0^{(1)}$	-.004209	.03506
$E_0^{(2)}$	-.01270	.02235
$E_0^{(3)}$	-.007726	.01463

Table 4: The central, Perturbation Value, column displays the correction terms calculated from perturbation theory. The Energy After Inclusion column shows the calculations from Equation 6.9, in a basis of seven, for perturbation theory corrections to harmonic oscillator energies for gravitons in the state  $L=2$  of different orders of correction.

Perturbation Order	Numerical Value	Energy After Inclusion
$E_0^{(0)}$	.03542	.03542
$E_0^{(1)}$	-.00829	.02713
$E_0^{(2)}$	-.00419	.02294
$E_0^{(3)}$	-.00344	.01950

Table 5: The central, Perturbation Value, column displays the correction terms calculated from perturbation theory. The Energy After Inclusion column shows the calculations from Equation 6.9, in a basis of seven, for perturbation theory corrections to harmonic oscillator energies for photons in the state  $L = 1$  of different orders of correction.

Perturbation Order	Numerical Value	Energy After Inclusion
$E_0^{(0)}$	.04671	.04671
$E_0^{(1)}$	-.008978	.03773
$E_0^{(2)}$	-.004530	.03320
$E_0^{(3)}$	-.003694	.02951

Table 6: The central, Perturbation Value, column displays the correction terms calculated from perturbation theory. The Energy After Inclusion column shows the calculations from Equation 6.9, in a basis of seven, for perturbation theory corrections to harmonic oscillator energies for photons in the state  $L=2$  of different orders of correction.

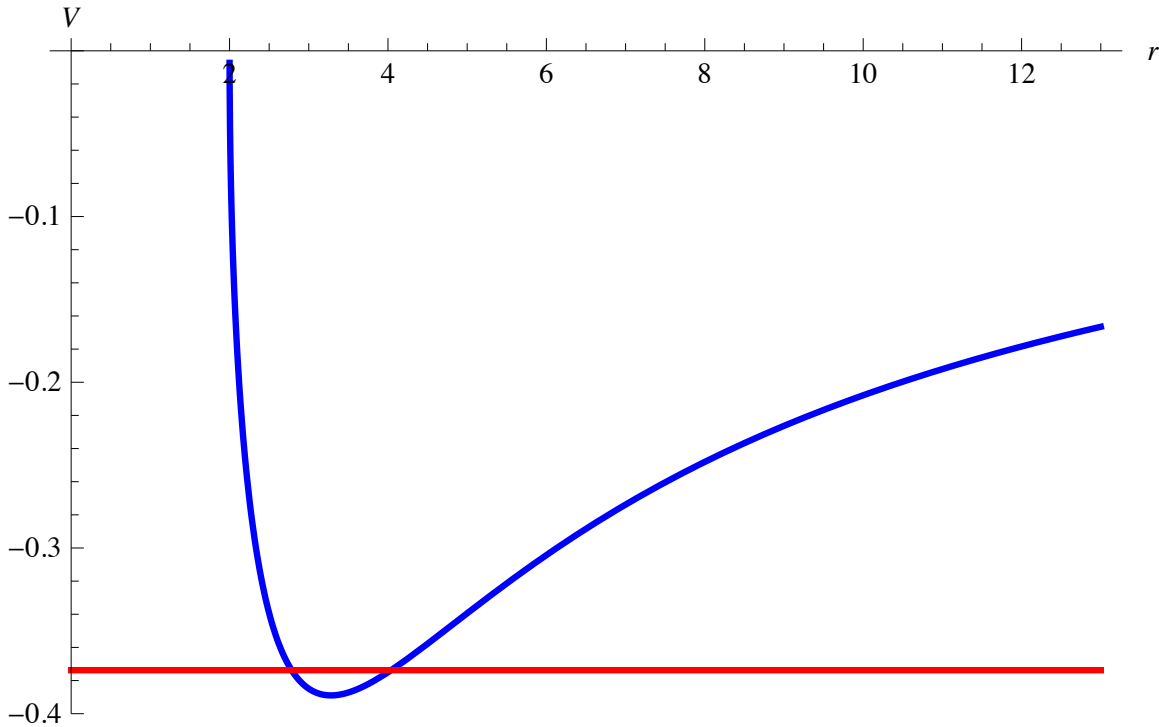


Figure 7: The Blue curve shows the effective potential energy curve for a graviton of  $L=2$ , calculated by the potential energy curve, Equation 6.2 on page 17. The Red line shows the location of the energy level calculated after the inclusion of the perturbation theory corrections up to the third order.

## 6.2 Properties of Trapped Photons and Gravitons

### 6.2.1 Photons

Photons are the particulate form of light. Though it is popularly understood that light exists as a wave, it is also experimentally seen that it exists in a particulate form. It is easier to think of this particle wave duality as the photon simply being the smallest iteration of a wave packet that can exist. This gives the photon a wave form, but a particulate nature. Photons carry electromagnetic energy.

Photons are zero rest mass particles, meaning that they do not exist unless they are moving at the speed of light. They are purely relativistic particles.

The spin of a particle can easily be calculated by observing what rotational angle over which the wave form of the particle is invariant. Equation 6.18 gives the spin for the particle with wave function that is invariant over the phase angle  $\theta$ . For photons, the wave function is invariant over a phase angle of  $2\pi$  indicating that the solution for  $s$  is 1; photons have spin 1. This comes from the dipole moment of the electric field, which causes a dipole nature in photons.

$$\theta = \frac{2\pi}{s} \tag{6.18}$$

The dipole moment and dipole nature of the photons comes as a result of the continuously oscillating electric field [24]. As the photon propagates, the electric field oscillates back and forth. The electric field can be thought of as continuously switching from positive to negative and back again. When the electric field moves from positive to negative and back again, it can be approximated as a positive and negative charge existing at the furthest part of the oscillation. This means that the

electric field acts like a dipole, creating a dipole moment for the electric field and therefore the photon. Since photons are the particulate form of the electric field, they can be thought of as having a dipole nature. This causes them to exist in only specific angular momentum states.

Particles and waves of spin 1 obey Bose-Einstein statistics. This property makes them bosons. Due to the statistical properties of bosons, more than one photon may exist in the same quantum state. Photons often exist in the lowest energy state in which they are able to exist.

Due to the zero rest mass of the photon, the kinetic energy of a photon is given by Equation 6.19, where  $h$  is Planck's constant and  $f$  is the frequency of the photon. For a photon in the cavity region, we calculate the period as  $7.29min$ , this gives a frequency of the wave to be  $2.28mHz$ .

$$E = hf \tag{6.19}$$

The kinetic energy of this wave is then calculated to be  $hf$ . Since Planck's constant is  $6.63 \times 10^{-34} \frac{m^2kg}{s}$ , that makes the energy of the photon equal to  $1.52 \times 10^{-36} J$ . This energy is negligible by comparison to the potential energy of the photons from being close to the black hole. For photons of  $L=1$ , that energy can be seen in Figure 3 on page 25 at the base of the photon potential energy curve. That energy has a unitless value of  $-.272$  which corresponds to a value in Joules, as converted by Table 1 on page 16, of  $-2.09 \times 10^{53} J$ . This means that the potential energy is on the order of  $10^{89}$  times larger than the kinetic energy of the waves.

It is possible for a wave function to remain stationary as the particle propagates. This is known as a standing wave. For a standing wave, the wave function does not

need to move in order for the particle to orbit. Since, in our case, the kinetic energy of the wave function is so low, these waves can be understood as standing waves. This means that all of their energy is contained in the potential energy due to the black hole interaction. This potential also influences the frequency of the standing waves. This is a difference from quantum mechanics, which utilizes the Virial Theorem to explain relations between kinetic and potential energy.

This causes a difference from classical and quantum mechanics, but this should not influence the calculations as long as we are aware of the implications this difference makes. The calculated wave function does not give the kinetic energy of the photon, but rather only the potential energy. This means that we are only working with the potential energy of the particle, rather than the connected kinetic and potential energies given by the Virial Theorem.

As was previously mentioned, the trapped photons exist in a leaky cavity. The calculations which we make from perturbation theory do not include the imaginary component to the energy as the data from the GR calculations do.

As will be shown for different values of  $L$  in section 6.4, the imaginary part of the frequency represents the stability of the orbit as having a proportionality to  $1/\tau$ , where the time,  $\tau$ , is the half-life. The imaginary part therefore is low for stable orbits and high for unstable orbits in time. This will be further expanded upon in section 6.4.

Photons do have an effective mass inside the cavity. They weakly interact gravitationally due to this effective mass, but the interaction is negligible compared to the interaction with the central black hole mass. Photons are uncharged, unlike electrons which contain a repulsive charge and higher mass. Consequently, each photon



contains its own wave function and energy that is independent of any other photon energy in the resonance state. Large numbers of photons can gather in this cavity due to the large energy preference to be in the lowest state coupled with the idea that the photon to photon gravitational interactions are negligible inside the cavity.

### 6.2.2 Gravitons

As of right now, the graviton is a theoretical particle that exists as the smallest wave packet possible of a gravitational wave. This is very similar to the photon, but exists for gravitational waves as opposed to electromagnetic waves.

Gravitons are zero rest mass particles, making them purely relativistic. Much like the photon with electromagnetic energy, gravitons carry gravitational energy [38]. Gravitational energy, unlike electromagnetic energy, has a quadrupole nature. This comes from the second order tensor nature of gravity. The polarization tensor, which is the linearization of the field equations, has two indices, which are symmetric. This gives the polarization tensor, which describes gravitational waves, the property of having a quadrupole moment [39]. The polarization tensor is also invariant over a phase shift of  $\pi$ , meaning that if we plug this into Equation 6.18 on page 35 for spin, we see that gravitons have a spin of 2.

The quadrupole moment, which causes the spin nature of the graviton, also influences its angular momentum and orbital states. Since the graviton has a zero rest mass, as with the photon, its mass cannot account for its spin properties. This means that the graviton cannot exist in any state with an angular momentum less than 2.

Gravitons have whole number spin, meaning that they obey Bose-Einstein statistics and can therefore exist in the same quantum state as other gravitons. This allows

the gravitons to collect in the lowest energy state since that is the most stable state (longest lifetime). Gravitons also obey the inclusion principle [23], meaning that the cavity of gravitons will attract other gravitons of the same frequency to become coherent with the cavity.

Since the gravitons are zero rest-mass particles, the kinetic energy of a graviton is given by Equation 6.19 on page 36. The graviton has a calculated period of  $4.84min$ . The frequency of the graviton in the cavity is  $3.44mHz$  based on this period. This means that the energy for a graviton in the cavity is  $2.28 \times 10^{-36}J$ . This is negligible compared to the potential energy of the graviton in the cavity, which is about  $-.389$ , as seen in Figure 5, or  $-3.00 \times 10^{53}J$ . This, as for the photon, indicates that the kinetic energy of the graviton is negligible. The graviton therefore exists in a standing wave.

Due to the energy being comprised of potential energy, the gravitons in the standing waves have the same general differences from classical and quantum mechanics that photons have, as discussed in the previous section.

### **6.3 How Angular Momentum Properties Influence the Orbitals**

Since the  $L=1$  state is the lowest state for photons, and photons are bosons which will gravitate toward the lowest energy state for the highest stability, we anticipate the majority of the trapped photons will exist in this state. This state in quantum mechanics relates to a P shaped orbital (P-orbital), as seen in Figure 8, which is an orbital with a zero probability at the nucleus. This is important since once a particle enters the black hole, it can never escape, meaning that if there is a probability for

the photon to exist in the center of the orbit, it could become absorbed by the black hole. This would remove it from the orbit and therefore from our resonance state. This would result in a different orbital stability. P-orbitals, on the other hand, offer a degree of stability for the orbit since the probability distribution drops to zero as the particle nears the center of the orbit. Photons cannot exist in an S shaped orbital since they cannot exist in an orbital that will prohibit their spin state. An electron, with spin  $1/2$  can exist in an S-orbital due to its nonzero rest mass, which can account for the spin state of the electron rather than the wave properties of the electron accounting for the spin state. Since photons have zero rest mass, their mass cannot account for their spin.

This idea, that the lowest lying photon state is a p-orbital, stems from the dipole nature of the electromagnetic waves of which photons are comprised. It limits their angular momentum to have a unitless value of 1, therefore confining them to a non-spherical distribution, such as a P-orbital around a black hole.

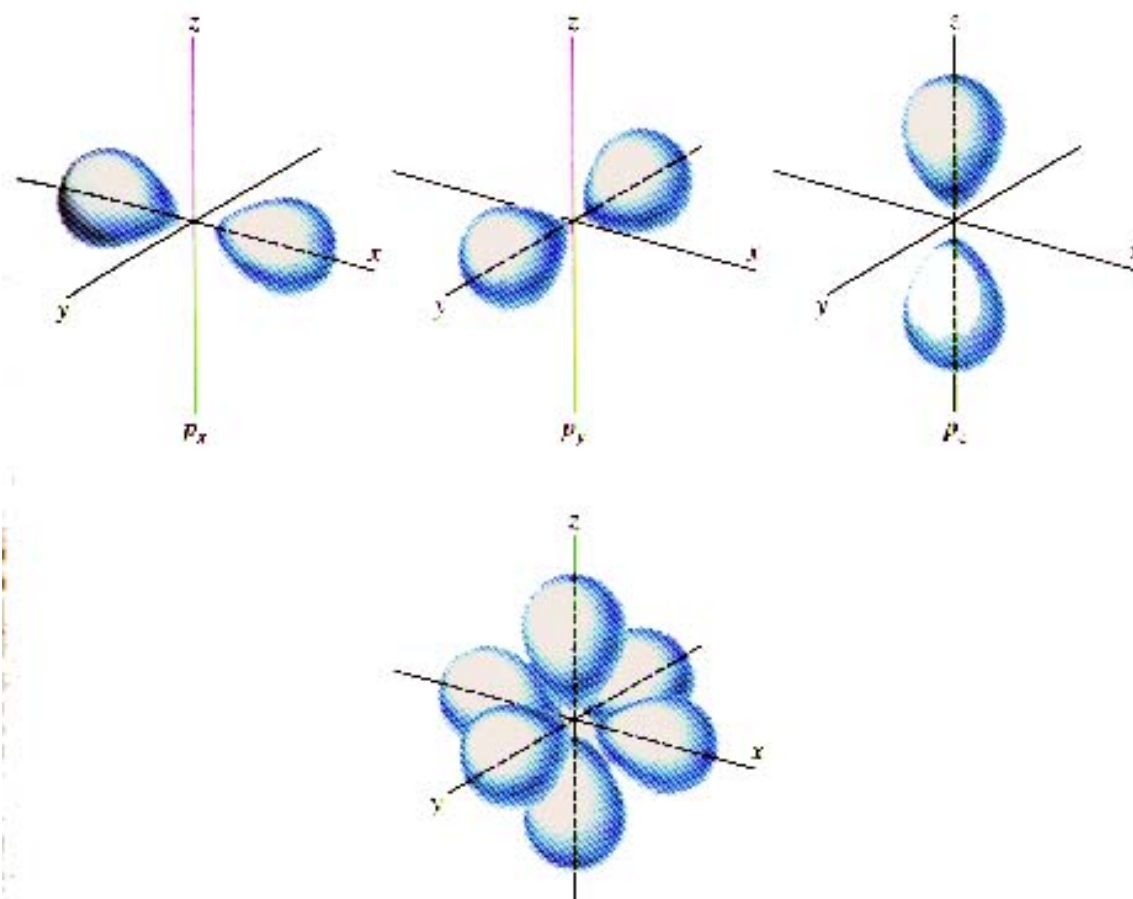


Figure 8: This shows the basic shape of a P-orbital from quantum mechanics. The Z-direction of the orbitals for a non-spinning black hole is defined by the magnetic field of the accretion disk. P-orbitals are the shape associated with  $L=1$  angular momentum states, the shape of the orbital photons in the lowest energy state. (This image was taken from <http://nanotech.sc.mahidol.ac.th/genchem/atom1/p-orb.jpg>)

In a similar manner, the quadrupole nature of the gravitational wave forces the graviton to have a lowest lying angular momentum of 2. This, in quantum mechanics, represents a D shaped orbital (D-orbital) for gravitons, as seen in Figure 9. D-orbitals also have a zero probability at the center of the orbit, indicating that there is no probability of the black hole absorbing the gravitons to remove them from their

resonance state.

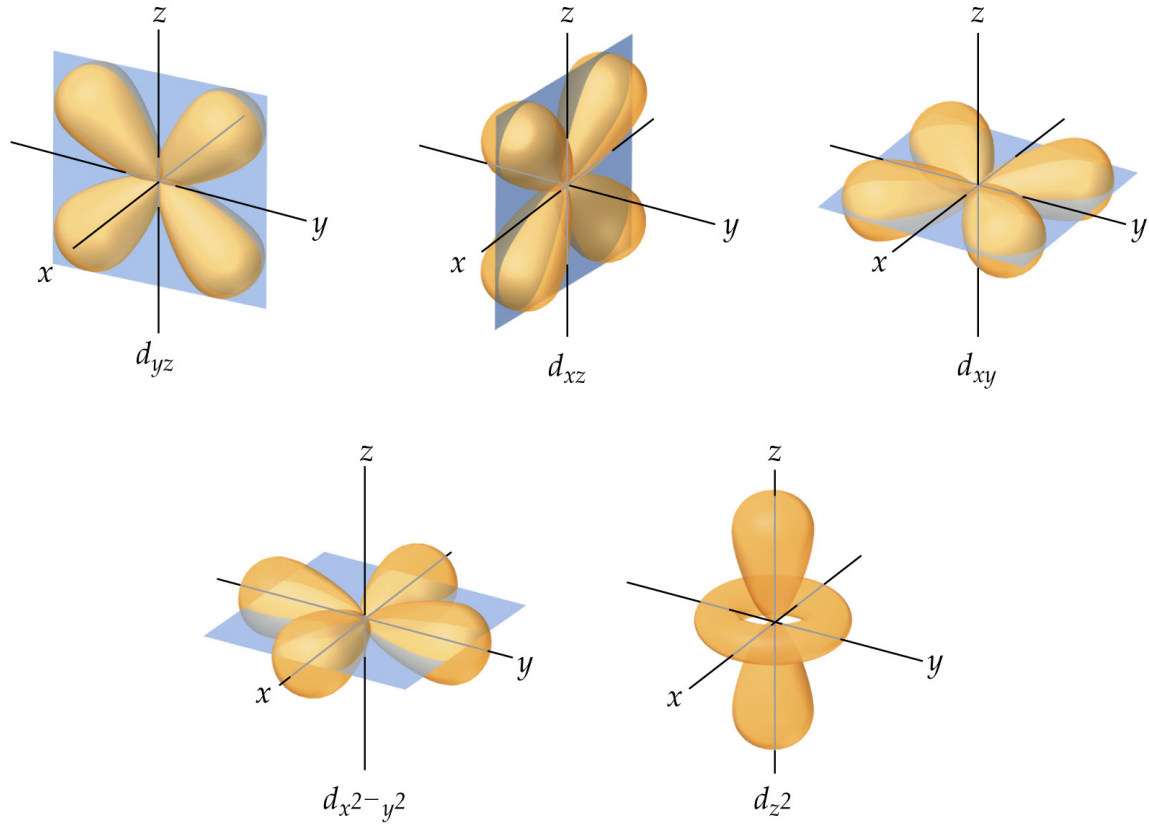


Figure 9: D-orbital shapes are typically the shape of  $L=2$  states in quantum mechanics. The Z-direction is defined by the magnetic field of the accretion disk for a non-spinning black hole. This is the shape of the orbital containing the most stable graviton state. (This image was taken from <http://chemistry.stackexchange.com/questions/2547/why-are-some-salt-solutions-coloured>.)

These orbitals compare to single electron orbitals, in hydrogen-like atoms, but in this case the photons and gravitons are bosons. In this comparison model, the mass of the black hole can be thought of as the net charge of the nucleus of the atom,

which is quantized, but the mass of the black hole is not quantized.

## 6.4 Most-Stable Energy States of Trapped Photons and Gravitons within the Cavity

Since photons and gravitons are bosons, and therefore obey the inclusion principle [23], they will collect in the lowest energy level state for their angular momentum. We did not calculate the frequency for different values of  $n$  due to this idea that in order to show our theory is accurate, the most populated, and therefore lowest energy, state should suffice to show that these particles exist in these energy states. We did conduct calculations for different angular momenta of the particles. This included calculations based on the three lowest angular momentum states for photons and for gravitons. These states are  $L=1, 2,$  and  $3$  for photons, and  $L=2, 3$  and  $4$  for gravitons.

We looked at these states since these are the most likely states in which states these bosons resonate. The  $L=1$  state for photons and  $L=2$  state for gravitons are the most likely state for those particles to resonate in due to the stability of the orbits at those levels. These are the orbits with lowest possible orbital angular momentum.

As previously mentioned, the potential energy in this region is often worked with as a  $V^2$  potential (Equation 6.1 on page 17). This potential, as seen in figure 1 on page 18 is a scattering potential. A scattering potential, as commonly seen with high energy particles above a potential barrier, can cause oscillations of the particles due to the changing difference in potential energy between a high potential region and low potential regions. The modes of these oscillations were calculated for this potential by Fröman et al. (1992) and Andersson (1992). They took the square root of their calculated values for the potential squared, which are presented in Table 7.

s	L	n	Real Part	Imaginary Part
1	1	0	.2483	-.09249
		1	.2145	-.2937
	2	0	.4576	-.09500
		1	.4365	-.2907
	3	0	.6569	-.09562
		1	.6417	-.2897
2	2	0	.3737	-.08896
		1	.3467	-.2739
	3	0	.5994	-.09270
		1	.5826	-.2813
	4	0	.8092	-.09416
		1	.7966	-.2843

Table 7: The square root of the normal modes calculated from the potential squared given by Equation 6.1 for different values of  $L$  and  $s$ . The  $n$  represents the  $n$ th mode for that iteration of  $L$  and  $s$ . States with  $n = 0$  and  $n = 1$  were included in this table but only  $n = 0$  states were calculated in this thesis. The  $n = 1$  states are shown to display the harmonic oscillator behavior of the scattering normal modes. A line has been placed between the  $s=1$  and  $s=2$  values to show the change from photon to graviton modes. These values were calculated by Fröman et al. [15].

This data is not comparable to our calculated values due to the fact that this energy is measured from a zero potential and ours is measured from the bottom of a potential well. Since the imaginary part of these values represent the stability of the leaky cavity, we only need to concern ourselves with matching results with the real part of the values. By subtracting the real part of these values from the bottom of our curves, we obtain a comparable value to our calculated results, shown in Table 8.

s	L	n	Numerical Value
1	1	0	.0239
		1	.0577
	2	0	.0138
		1	.0349
	3	0	.0098
		1	.0250
2	2	0	.0152
		1	.0421
	3	0	.0101
		1	.0269
	4	0	.0072
		1	.0198

Table 8: The real part of the square root of the normal modes calculated from the potential squared given by Equation 6.1 for different values of  $L$  and  $s$  from Table 7 as measured from the bottom of our potential wells. These values were calculated by subtracting the real part of the values in Table 7 from the magnitude of the potentials at the bottom of the wells, seen in Figure 2 on page 20 for photons and gravitons.

After measuring the values from the bottom of our potential curves, it is clear that the normal mode for the  $L=2$  state of the graviton is at the same energy as the value from the perturbation theory calculations, in Table 4 on page 33. The potential energy curves as calculated from non-relativistic quantum mechanics agree with the calculated values of the normal modes from GR.

The energy values from the normal modes show a nature of a harmonic oscillator potential, not just from our calculated results, but also due to the relationship between different levels of  $n$ . In the harmonic oscillator, the discrete energy levels have whole number separation starting at  $1/2$ . The  $n = 1$  state is 3 times the energy of the  $n = 0$  state. The same pattern is seen when we treat the normal modes in Table 8 as being energy eigenstates from a potential well. This pattern continues for many



of the calculated values of  $n$ , but as  $n$  increases, due to the widening of the potential compared to the harmonic oscillator potential, the intervals stray farther and farther from the harmonic oscillator values. As the energy and radius increases, the levels approach one another until they coalesce into a single blurred state. For large  $n$ , this becomes very similar to how the energy levels of Hydrogen-like atoms behave.

If we wish to compare the energy values from our perturbation calculations with these values from the scattering potential, we need to change the calculated values from perturbation theory to ones measured from zero as opposed to ones measured from the bottom of the curve. Table 9 shows the value from the normal mode of the scattering potential with the value calculated from the third order perturbation correction and the error between them. These values matched within 4% error, indicating that our perturbation theory calculations nearly match the normal mode calculations from the scattering potential.

s	L	Value from Scattering Potential	Value from Perturbation Theory	Percent Error
1	1	.2483	.2439	1.77%
	2	.4576	.4733	3.43%
2	2	.3737	.3731	.161%

Table 9: The real part of the normal modes represent the energy of the state. These values are comparable to our calculated values when those values are measured from the zero energy line as opposed to the shifted potential we used when comparing to the harmonic oscillator. In order to calculate the energies of our perturbation theory corrections, the values were added to the bottom of the curve presented in Figure 2 on page 20.

As mentioned previously, the imaginary part of the energy and frequency relates to the stability of the orbit. The value of the imaginary part is proportional to  $1/\tau$  (where  $\tau$  is the half-life time); therefore, the larger the imaginary part of the energy,

the more unstable the orbit.

As seen in Table 7 on page 44, the imaginary parts of the  $n = 1$  states are much larger than the imaginary parts for the  $n = 0$  states. The  $n=1$  states are much less stable than the  $n = 0$  states. The  $n=1$  states are then, much less populated.

The  $n = 0$  states all have comparable stability, since the lowest angular momentum states have the lowest imaginary values. We calculated the stability of the states in average number of cycles by dividing the real part, which is proportional to the frequency, by the imaginary part. The results of this are shown in Table 10.

s	L	Average Number of Cycles
1	1	2.685
	2	4.817
	3	6.870
2	2	4.201
	3	6.466
	4	8.594

Table 10: The number of average cycles for the lifetime of the orbitals to show the stability of each orbital based on number of cycles. These values were calculated from the real and imaginary parts of the normal modes of the scattering potential, seen in Table 7.

The time-based stability is important for consideration because the states with the best time-based stability will be the highest populated states. This corresponds to the  $L=1$  state for photons and the  $L=2$  state for gravitons. The stability in terms of cycles shows how deep the potential energy wells are and how stable the orbits are based on the deep curvature of the potential well. As is clear by Figure 3 and Figure 4 on pages 25 and 26, the potential wells become deeper for higher values of  $L$ , corresponding to more average cycle stability in terms of time for one orbit. This

nature is confirmed by the normal mode stability by Table 10.

## 6.5 Photon and Graviton interaction with Electrons in the Cavity Region

Electrons emit synchrotron radiation by being accelerated. When electrons orbit an object, they are experiencing a centripetal acceleration causing them to emit synchrotron radiation. This radiation intensity is based on the density and volume of the electrons which are accelerated.

Electrons can form into high density “blobs” by interaction with photons or gravitons. These blobs emit more radiation due to their higher density. Photons, which are made up of electromagnetic radiation, interact with electrons based on the electron’s charge. Photons that are in the same state have their electric field lined up, which acts upon nearby electrons. The photons will oscillate, causing the electron density to oscillate at the same frequency as the photons. This allows us to see the photon frequency by the oscillating intensity of the electron emission.

The emission intensity is complicated by the volume of the blob oscillations, thermal fluctuations, magnetic field variations and further density oscillations. We did not fully investigate these interactions, since that involves calculations and understanding beyond the scope of this work, but it is theorized that the emission from these electrons should be heavily dependent on the density of the electron blobs caused by the electron-photon interaction.

The gravitons interact with the electrons based on the mass of the electrons. This causes a similar reaction of the electrons as in photons, but instead of grouping together based on charge, they group based on mass. Blobs of electrons form and emit

radiation in a similar manner to the photon-electron interaction, but in this case the electron emission fluctuations follow the pattern set by the gravitons. The graviton oscillations are then visible through the electron emissions. Like the photon interaction, this is also further complicated by thermal, magnetic, and volume oscillations and instabilities.

In order to observe the photon and graviton cavity resonances, we must observe the electron interactions with the cavity from the electron emissions. For this, we looked at NIR non-thermal electron emissions near a black hole.

## 7 Choosing a Black Hole to Observe [4]

Since our theory, due to our unit system, is valid for all black holes, it does not technically matter which black hole we look at to find data to support it. The selection for the black hole is then based on which black hole has the largest luminosity, and therefore gives the best signal to study, as seen from earth. There are many candidates for large or close black holes but we wanted to look at the one with the highest apparent brightness in order to get larger intensities and lower the influence of background noise.

The black hole in the center of our galaxy, Sagittarius A\*(Sgr A\*) has a mass of about  $3.7 \times 10^6 M_{\odot}$  and is about  $2.6 \times 10^4 ly$  away. Some quick calculations can show that other reasonable candidates for bright black holes are not as apparently bright as Sgr A\*, making Sgr A\* the primary black hole to be observed to confirm the existence of the aforementioned resonance states.

We looked at the black hole with the highest absolute brightness in the virgo cluster, a large galactic cluster near the local group. The aforementioned galaxy at the center of the virgo cluster, M87, is a supergiant elliptical galaxy believed to have been created by the collision and merging of several spiral galaxies. The supermassive black hole at the center of M87 is about  $6 \times 10^9 M_{\odot}$  and is about  $5.3 \times 10^7 ly$  away from earth. Since the luminosity of a black hole is based on mass and luminosity scales on distance as  $1/r^2$  we can compare the luminosity at earth to the luminosity of Sgr A\* by looking at the ratio of the mass and the ratio of the distances squared. The mass ratio of the black hole in M87 with Sgr A\* is about  $1.6 \times 10^3$  while the squared distance ratio is about  $2.4 \times 10^{-7}$ . We multiply these ratios to see that the black hole in M87 has about  $3.9 \times 10^{-4}$  times the luminosity of Sgr A\* at earth. This

means that Sgr A\* is a better source to observe than the black hole in M87.

The Andromeda galaxy is the closest galaxy with a central black hole to the Milky Way. This means that it is close enough that it could contain a black hole sufficiently massive to be more apparently luminous than Sgr A\*. At a mass of  $3 \times 10^7 M_{\odot}$  and distance of  $2.5 \times 10^6 ly$ , the black hole in the Andromeda galaxy is about  $8.76 \times 10^{-4}$  times the apparent luminosity of Sgr A\*. It is not more apparently luminous than Sgr A\*. This indicates that we should not look at extragalactic black holes, since both the largest and the closest were not more apparently luminous than Sgr A\*.

Since intermediate-mass black holes have not yet been observed, we ignore them as a possibility for data collection. We looked at a large, close stellar mass black hole A0620-00/V616 Mon which has a mass of  $11 M_{\odot}$  at a distance of  $3500 ly$ . This means that it is about  $1.6 \times 10^{-4}$  times the apparent luminosity of Sgr A\*, making it less suitable for observation.

This takes into account all possible types of confirmed black holes for observation and has shown that Sgr A\* is the best black hole to be observed. Since visible light from the observation of Sgr A\* is absorbed by dust, it is best to observe in NIR, infrared and x-ray wavelengths, which are absorbed less because average dust particles are usually the size of visible wavelengths, rather than NIR, infrared or x-ray wavelengths.

## 8 Observing the Black Hole Sgr A\*

Using adaptive optics, it is possible to distinguish the NIR emissions from nearby stars from the emission due to particles extremely close to the black hole. When looking at this NIR spectrum ??, there are noticeable spikes in radiation about 4 times a day that last about an hour. These flares are accompanied by 20 minute subflares. Observed with these flares and subflares there appears to be a noticeable, continuous, varying signal, present when the black hole is not flaring. The idea of a continuously varying oscillation is substantiated by best fit models for the flux distributions showing that Sgr A\* has an active NIR spectrum more than 40% of the time, as explained by Dodds-Eden et al. [7].

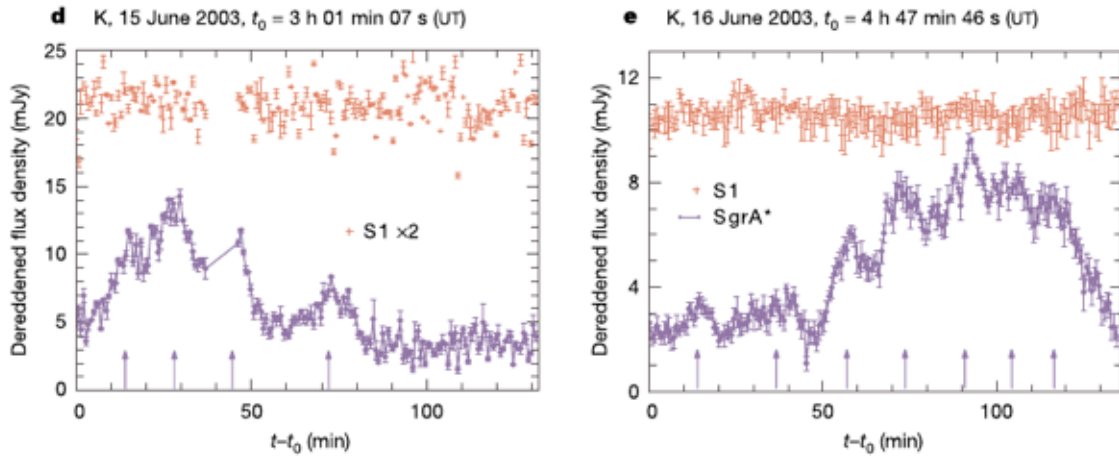


Figure 10: This is the NIR data from the 2003 article by Genzel et al [16]. It clearly shows two separate NIR flares, each with subflares. The continuously varying oscillations are visible when looking at the signal when the flare stops or on top of the flares and subflares. For example, these oscillations can be clearly seen when the flares are less prominent, as in the last 50min of the data taken on 15 June 2003 and in the first 40min of the 16 June 2003 data. This data was taken in the  $K_s$  band (wavelength between 2 and 4  $\mu\text{m}$ ) of NIR, and the article by Genzel et al makes note that it contains signal even during quiescent emissions (between flaring events). Reprinted by permission of Macmillan Publishers Ltd: Nature Magazine [16], copyright 2007.

## 8.1 NIR and X-Ray Flares

As previously mentioned, there are observed NIR flares coming from the area very close to the black hole Sgr A\*. These flares and subflares are classified as Quasi-Periodic Oscillations (QPOs), meaning that they do not have a stable period.

The primary NIR flares happen about 4 times a day and about once a day are accompanied by an X-ray flare. The X-ray flare always accompanies a NIR flare but the NIR flares can exist without the X-ray flare. These flares each last about an hour to 80 minutes in time. The NIR flares contain a riding subflare which has a period of about 20 minutes, but this period can range from 13-30 minutes between



each subflare [7].

Little is known about these flares or subflares, but there are some competing theories as to what causes them. For the purpose of this research, the cause of the flares and subflares is not important and so it will not be explained in much detail. We will instead focus on the continuous variability of the NIR signal.

### **8.1.1 Possible Explanations for Flares and Subflares**

As of right now the literature contains varying ideas as to what can cause the NIR flares and/or subflares but there has been no observational confirmation of any of the competing theories. One such theory was the idea of a “hot blob” that was orbiting the black hole very rapidly. There are some other theories as to what mechanism can cause these kind of flares. The paired X-ray and NIR flares can possibly be due to synchrotron emission and submm photons due to inverse Compton scattering by the NIR-emitting electrons. They can also be due to self Compton effects, or cooling break synchrotron emission [8].

The data concerning flares and subflares has been put through self correlating and power density functions to show that these occur within certain degrees of confidence, but it is still unknown what phenomenon is causing these emissions.

## **8.2 Possible Causes of the Continuous Variability Signal**

No article in the literature has provided a model or idea to explain the existence of a constantly varying source around the black hole beyond vague statements, such as that it may have something to do with interactions with thermal electrons or something to do with the interaction from the accretion disk [7]. These short and

unexplained ideas do not provide sufficient information to account for the oscillations. The accretion disk is too distant from the black hole to create an oscillation of this speed. Many articles choose to ignore this varying signal or attribute it to noise, even though there is no known form of noise to account for it and it is very regularly oscillating below the Nyquist frequency for the data taken. Some articles, including Dodds-Eden et al. [8] [7], have mentioned that determining what is causing the emission is a “difficult question.” The NIR spectrum is coming from non-thermal, synchrotron, electron emission based on wavelength, and it has not been determined what is causing the NIR intensity to vary in this way.

This continued variability is also different from any stellar observation to this date. It was noted by Dodds-Eden et al. [7] that these variations were significantly more intense than variations of stars with comparable flux. This indicates that it is not likely to be variations caused by a nearby star and that it is not being caused by a process that normally exists in stellar objects. Black holes must contain some process or phenomenon that causes these oscillations that does not exist in less dense objects.

As to our knowledge, no one has published anything on the oscillations from the gravitational cavity or regarding any phenomenon that exists closer than the accretion disk. This will be the first detailed explanation for the existence of the continued variability signal present in the NIR spectrum of the black hole Sgr A\*.

### **8.2.1 Our Theory Explains the Continuous Variability of Sgr A\***

The continuously varying NIR signal, according to our calculations, is due to the resonance cavities for standing wave photons and gravitons and their interaction with

electrons within the cavity region.

The NIR flare data is presented in Figure 10 on page 53 and Figure 11. As seen in Figure 11, the times of the oscillations matches well with observed fluctuations in the NIR spectrum.

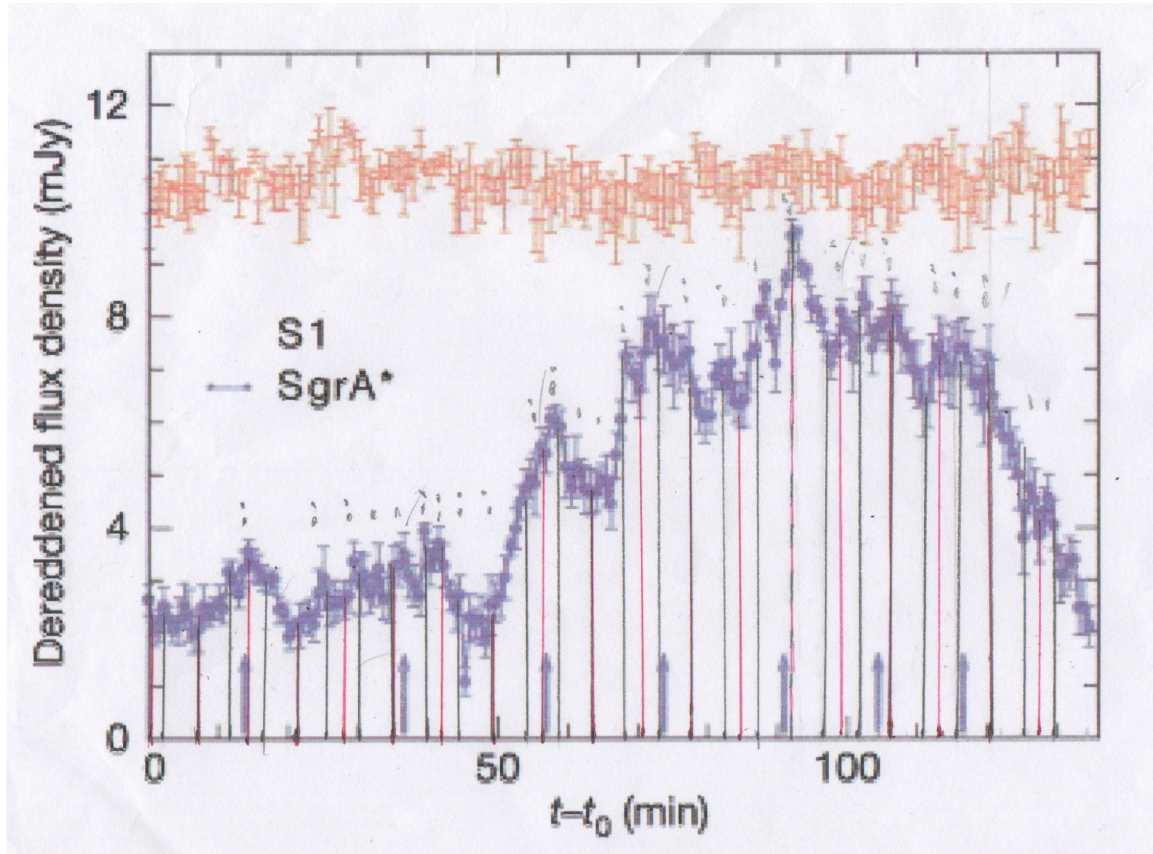


Figure 11: The NIR data from Figure 10 plotted with lines representing the corresponding times for electron emissions due to photon and graviton resonances. We used the June 16th data since the June 15th data had lower signal to noise ratio and was missing data for certain times. The June 15th data does seem to convey the same pattern, which lines up well with the June 16th data presented here for continuous emission signals. The Red lines represent the oscillations due to the lowest photon resonance and the Grey lines represent the oscillations due to the lowest graviton resonance. Notice how these lines seem to correspond to small peaks in the NIR data.

Usually the validity of an oscillatory structure is given by a power density spectrum, but due to the flare and subflare nature of the data, the power density spectrum of the signal is sometimes buried by the competing flare and subflares. The analysis of Figure 10 was done by hand due to the difficulty of creating a power spectrum on the data. The continuous variability signal is sometimes buried by other signals, possibly for entire cycles. The signal intensity depends on the number of electrons in blobs and the number of bosons in the coherent state, which both vary. The frequency is dependent upon physical size of the cavity and character of the electromagnetic or gravitational wave, but does not depend upon the number of electrons in blobs nor the number of bosons in the resonant state. The variations in the signal intensity combined with the overriding flare and subflare signals creates difficulty in obtaining a power spectrum of the resonant states since they are often buried beneath the flares or subflares for several cycles.

The periods, obtained by hand for Figure 10 on page 53 and illustrated in Figure 11 on page 56, for the lowest lying, and most stable, energy states for photons and gravitons were 7.29 minutes and 4.84 minutes, respectively. These coincide well with the continuously varying NIR oscillations.

In order to obtain a proper power density spectrum, we need to look at data from the NIR spectrum of the black hole when it is not flaring. In this situation the only present signal should be due to the continuously varying signal, at the resonant photon and graviton frequencies. This should allow a power density spectrum so be obtained, without interference from other sources of variation due to the complex situation in the region immediately surrounding the black hole, including the accretion disk.

The inability to obtain a power density spectrum also makes it impossible to

obtain a confidence interval value for the fit of the oscillations with our theory, but once a power density spectrum is obtained for data obtained when the black hole is not flaring, we will be able to obtain a confidence interval value for these oscillations.

We hope to be able to obtain non-flaring NIR data although this inter-flare period is less interesting to scientists who obtain observational data. We are confident that the statistical analysis of such data will provide a more direct observable proof of our theoretical work. Our current analysis has pointed us in the direction needed to more fully work with Sgr A\* data emanating from low frequency photon and graviton resonance states in the gravitational cavities surrounding any black hole.

## 9 The Importance of Measuring a Graviton

The graviton is still considered a theoretical particle. There has never been an observational or experimental proof of the existence of the graviton. Gravitational waves were recently indirectly observed by Hulse and Taylor [12], making the hunt for a way to prove the graviton's existence on the forefront of scientific exploration. The graviton is a particle predicted by GR, which makes its existence another indication that Einstein was correct about his theory of GR.

This work provides theorems that are rooted in the GR properties of the graviton. By studying the NIR continuous variability when the black hole Sgr A\* is not flaring, we can observe that the 4.84 minute period of the oscillations are caused by the most stable graviton resonance state ( $L=2$ ). With continued exploration based on these oscillations, the boson properties of gravitons may be seen as the only possible explanation for this phenomenon. This would lay the framework for showing that gravitational waves have a particulate form.

Proving the existence of the graviton, with the assumed resonant cavity properties, would provide insight into GR. The orbital nature of the photon and graviton resonance states in the cavity near a black hole has been emphasized in this thesis.

## 10 Conclusions

We have used non-relativistic quantum mechanical techniques to approximate some general relativistic resonant properties near the event horizon of a black hole. This showed that there are low energy photon and graviton resonance states around the exterior of a black hole bound by a gravitational potential. The lowest energy states show some similarities to particles in the quantized states of a harmonic oscillator. The orbital angular momentum of these states show properties reminiscent of the orbital angular momenta of electrons in Hydrogen-like atoms.

The brightest emitter of NIR radiation in our galaxy is the Supermassive Black Hole at the center, Sgr A\*. Our work reveals the cause of the observed constant NIR oscillations which are present. The NIR radiation gets brighter and darker in periods of 7.29 minutes due to the lowest photon resonance and 4.85 minutes due to the lowest graviton resonance interacting with electrons as the electrons approach the black hole. The lifetimes of these resonances are longer than any other resonance of this type. They are also more densely populated, indicating that these lowest energy states heavily influence electrons in the cavity region surrounding a black hole.

We show that our predictions of the resonance states of photons and gravitons from the Supermassive Black Hole match nicely with observed continuously varying oscillations seen when observing the Quasi-Periodic Oscillations (QPOs) of NIR signals measured at Earth from Sgr A\*.

The Theory of General Relativity predicts that gravitational waves travel at the speed of light. In the region near a black hole at the correct distance, gravitational waves circle it, influencing the radiation emitted by falling material within that region. Our work reveals the resonance properties at certain frequencies of these gravitons.

The same holds true for photons orbiting the black hole at the correct distance for photon resonance. Large numbers of gravitons and photons may be coherent, having not only the same frequency but also phase and direction. Within sufficient number of gravitons and/or photons in the same resonant and coherent states, bunches of electrons can be influenced jointly, emitting radiation at the same frequencies as the resonant photons and gravitons.

Once spin is introduced into the equations, we expect to be able to show that gravitons move at the same, constant speed of light ( $2.998 \times 10^8$  m/s) in a strong gravitational environment. This can be tested by comparing the data to the experimental results of QPO/NIR data from Sgr A\*. This would be a proof of general relativity rooted in experimentally observed data. Our work presented herein is valid for all Schwarzschild black holes, whether large or small.

Our future work is planned to include: (1) How the electrons accumulate into blobs of certain density and volume, including how this changes the intensity of radiation emitted from these blobs. Naturally, the motion of the blobs depends on the electric and gravitational fields of large numbers of coherent photons and gravitons and their respective frequencies. (2) The theoretical (GR) prediction of the influence of black hole spin on the surrounding photon and graviton orbitals and resonant frequencies. (3) The confirmation of the existence of the influences predicted by GR in the observational data from the supermassive black hole situated at the center of the Milky Way Galaxy.



## References

- [1] Nils Andersson. A numerically accurate investigation of black-hole normal modes. *Proc. R. Soc. London*, 439:47–58, May 1992.
- [2] D.R. Bates, editor. *Quantum Theory*. Academic Press, 1961.
- [3] Carl M. Bender. Perturbation theory in large order. *Advances in Mathematics*, 30:250–267, 1978.
- [4] Bradley W. Carroll and Dale A. Ostlie. *Introduction to Modern Astrophysics*. Pearson Education, Inc, second edition edition, 2007.
- [5] S. Chandrasekhar. *The Mathematical Theory of Black Holes*. Clarendon Press - Oxford, 1992.
- [6] Stephen J. Crothers. On the Regge-Wheeler Tortoise and the Kruskal-Szekeres coordinates. *Progress in Physics*, 3:30–34, 2006.
- [7] K. Dodds-Eden, S. Gillissen, T.K. Fritz, F.Eisenhauer, S. Trippe, R. Genzel, T. Ott, H. Bartko, O. Pfuhl, G. Bower, A. Goldwurm, D. Porquet, D. Proquet, G. Trap, and F. Yusef-Zadeh. The two states of Sgr A\* in the near-infrared: bright flares on top of low-level continuous variability. *Astrophysical Journal*, 728(37):1–14, February 2011.
- [8] K. Dodds-Eden, D. Porquet, G. Trap, E. Quataert, S. Gillessen, N. Grosso, R. Genzel, A. Goldwurm, F. Yusef-Zadeh, S. Trippe, H. Bartko, F. Eisenhauer, T. Ott, T.K. Fritz, and O. Pfuhl. Flares from Sgr A\* and their emission mechanism. *ASP Conference Series*, 2010.

- [9] K. Dodds-Eden, D. Porquet, G. Trap, E. Quataert, X. Haubois, S. Gillissen, N. Grosso, E. Pantin, H. Falcke, D. Rouan, R. Genzel, G. Hasinger, A. Goldwurm, F. Yusef-Zadeh, Y. Clenet, S. Trippe, P.-O. Lagage, H. Bartko, F. Eisenhauer, T. Ott, T. Paumard, G. Perrin, F. Yuan, T.K. Fritz, and L. Mascetti. Evidence for x-ray synchrotron emission from simultaneous mid-infrared to x-ray observations of a strong Sgr A\* flare. *Astrophysical Journal*, 698:676–692, June 2009.
- [10] S. Doeleman, J. Weintroub, A. E. E. Rogers, R. Plambeck, R. Freund, R. P. J. Tilanus, Per Friberg, L. M. Ziurys, J. M. Moran, B. Corey, K. H. Young, D. L. Smythe, M. Titus, D. P. Marrone, R. Cappallo, D. C.-J. Bock, G. C. Bower, R. Chamberlin, G. R. Davis, T. P. Kirchbaum, J. Lamb, H. Maness, A. E. Niell, A. Roy, P. Strittmatter, D. Werthimer, A. R. Whitney, and D. Woody. Event-horizon-scale structure in the supermassive black hole candidate at the galactic centre. *Nature*, 455:78–80, September 2008.
- [11] J. C. Dolence, C. F. Gammie, H. Shiokawa, and S. Noble. Near-infrared and x-ray quasi-periodic oscillations in numerical models of Sgr A\*. *Astrophysical Journal*, 746(L10), January 2012.
- [12] Gösta Ekspong, editor. *Nobel Lectures in Physics, 1991-1995*. The Nobel Foundation, March 1997.
- [13] Herbert Friedman. *The Astronomer's Universe*. W.W. Norton and Company, 1990.

- [14] T. Fritz, S. Gillissen, S. Trippe, T. Ott, H. Barko, O. Pfuhl, K. Dodds-Eden, R. Davies, F. Eisenhaur, and R. Genzel. What is limiting near-infrared astronomy in the galactic centre. *Monthly Notes of the Royal Astronomical Society*, 401:1177–1188, 2010.
- [15] Nanny Fröman, Per Olof Fröman, Nils Andersson, and Anders Hökback. Black-hole normal modes: Phase-integral treatment. *The American Physical Journal*, Physical Review D:2609–2616, April 1992.
- [16] R. Genzel, R. Schödel, T. Ott, A. Eckart, T. Alexander, F. Lacombe, D. Rouan, and B. Aschenbach. Near-infrared flares from accreting gas around the super-massive black hole at the galactic centre. *Nature*, 425:934–937, October 2003.
- [17] S. Gillessen, R. Genzel, F. Eisenhauer, T. Ott, S. Trippe, and F. Martins. 15 years of high precision astronomy in the galactic center. *International Astronomy Union Symposium*, 248:466–469, 2007.
- [18] David Griffiths. *Quantum Mechanics*. Pearson Prentice Hall, second edition, 1995.
- [19] S.W. Hawking and W. Israel, editors. *300 Years of Gravitation*. Cambridge University Press, 1897.
- [20] Walter David Jackson. *Classical Electrodynamics*. John Wiley and Sons, Inc, third edition, 1962.
- [21] Max Jammer. *The Conceptual Development of Quantum Mechanics*, volume 12. Tomash Publishers, 1989.

- [22] G. Kaniadakis. Generalized Boltzmann equation describing the dynamics of bosons and fermions. *Physical Letters A*, 203:229–234, July 1995.
- [23] G. Kaniadakis and P. Quarati. Classical model of bosons and fermions. *Physical Review E*, 49(6):5103–5110, June 1994.
- [24] Robert B. Leighton. *Principles of Modern Physics*. McGraw-Hill Book Co. Inc., 1959.
- [25] Ira N. Levine. *Quantum Chemistry*. Allyn and Bacon, Inc., second edition, 1970.
- [26] Eugen Merzbacher. *Quantum Mechanics*. John Wiley and Sons, Inc, 1961.
- [27] Charles Misner, Kip S. Thorne, and John A. Wheeler. *Gravitation*. W.H. Freeman and Company, 1970.
- [28] M. Moscibrodzka, H. Shiokawa, C. F. Gammie, and J. C. Dolence. The galactic center weather forecast. *Draft*, 2012.
- [29] Hans C. Ohanian and Remo Ruffini. *Gravitation and Spacetime*. W.W. Norton and Company, second edition, 1976.
- [30] R.V. Pound and G.A. Rebka Jr. Apparent weight of photons. *Physical Letters*, 4(337), April 1960.
- [31] Wesley C. Salmon, editor. *Zeno’s Paradoxes*. Hackett Pubb Co Inc, 2001.
- [32] R Schödel, M.R. Morris, K. Muzic, A. Alberdi, L. Meyer, A. Eckart, and D.Y. Gezari. The mean infrared emission of Sagittarius A\*. *Astronomy and Astrophysics*, pages 1–14, June 2011.

- [33] Michael A. Seeds. *Foundations of Astronomy*. Thomson Brooks/Cole, ninth edition, 2007.
- [34] R. Shankar. *Principles of Quantum Mechanics*. Springer, second edition, 1980.
- [35] Roman Shcherbakov and Jonathan C. McKinney. Submillimeter quasi-periodic oscillations in magnetically choked accretion flows models of Sgr A\*. *Draft*, 2013.
- [36] Edwin F. Taylor and John A. Wheeler. *Exploring Black Holes*. Addison Wesley Longman, Inc., 2000.
- [37] S. Trippe, T. Paumard, S. Gillessen, T. Ott, F. Eisenhauer, F. Martins, and R. Genzel. Near-infrared observations of Sagittarius A\*. *RevMexAA Serie de Conferencias*, 32:12–14, 2008.
- [38] Robert M. Wald. *General Relativity*. The University of Chicago Press, 1984.
- [39] Steven Weinberg. *Gravitation and Cosmology Principles and Applications of the General Theory of Relativity*. John Wiley and Sons, Inc, 1972.

# Appendices

## A Additional Tables

Harmonic Oscillator Eigenvalue	Numerical Calculation
$E_0^{(0)}$	.0531
$E_1^{(0)}$	.159
$E_2^{(0)}$	.266
$E_3^{(0)}$	.372
$E_4^{(0)}$	.478
$E_5^{(0)}$	.585
$E_6^{(0)}$	.691

Table 11:  $E_n^{(0)}$  terms for perturbation theory corrections for harmonic oscillator wave functions in the harmonic oscillator potential for gravitons in the state  $L=3$ .

Harmonic Oscillator Eigenvalue	Numerical Calculation
$E_0^{(0)}$	.0591
$E_1^{(0)}$	.177
$E_2^{(0)}$	.295
$E_3^{(0)}$	.414
$E_4^{(0)}$	.532
$E_5^{(0)}$	.651
$E_6^{(0)}$	.769

Table 12:  $E_n^{(0)}$  terms for perturbation theory corrections for harmonic oscillator wave functions in the harmonic oscillator potential for gravitons in the state  $L=4$ .

Harmonic Oscillator Eigenvalue	Numerical Calculation
$E_0^{(0)}$	.0355
$E_1^{(0)}$	.106
$E_2^{(0)}$	.177
$E_3^{(0)}$	.248
$E_4^{(0)}$	.319
$E_5^{(0)}$	.390
$E_6^{(0)}$	.461

Table 13:  $E_n^{(0)}$  terms for perturbation theory corrections for harmonic oscillator wave functions in the harmonic oscillator potential for photons in the state L=1.

Harmonic Oscillator Eigenvalue	Numerical Calculation
$E_0^{(0)}$	.0467
$E_1^{(0)}$	.140
$E_2^{(0)}$	.234
$E_3^{(0)}$	.366
$E_4^{(0)}$	.420
$E_5^{(0)}$	.513
$E_6^{(0)}$	.607

Table 14:  $E_n^{(0)}$  terms for perturbation theory corrections for harmonic oscillator wave functions in the harmonic oscillator potential for photons in the state L=2.

Harmonic Oscillator Eigenvalue	Numerical Calculation
$E_0^{(0)}$	.0555
$E_1^{(0)}$	.167
$E_2^{(0)}$	.278
$E_3^{(0)}$	.389
$E_4^{(0)}$	.500
$E_5^{(0)}$	.611
$E_6^{(0)}$	.722

Table 15:  $E_n^{(0)}$  terms for perturbation theory corrections for harmonic oscillator wave functions in the harmonic oscillator potential for photons in the state L=3.

Wave Function	$ U_0 \rangle$	$ U_1 \rangle$	$ U_2 \rangle$	$ U_3 \rangle$	$ U_4 \rangle$	$ U_5 \rangle$	$ U_6 \rangle$
$\langle U_0  $	-.00967	-.0238	-.0242	-.00321	-.00941	.00204	.00223
$\langle U_1  $	-.0238	-.0439	-.0392	-.0607	-.00186	-.0156	.00261
$\langle U_2  $	-.0242	-.0392	-.101	-.0484	-.104	.000126	-.0207
$\langle U_3  $	-.00321	-.0607	-.0484	-.171	.0542	-.151	.00225
$\langle U_4  $	-.00941	-.00186	-.104	.0542	.250	-.0580	-.200
$\langle U_5  $	.00204	-.0156	.000126	-.151	-.0580	-.334	-.0604
$\langle U_6  $	.00223	.00261	-.0207	.00225	-.200	-.0604	-.421

Table 16:  $dV_{nm}$  terms for perturbation theory for various combinations of wave functions and difference between the harmonic oscillator and our calculated potential for gravitons in the L=3 state.

Wave Function	$ U_0 \rangle$	$ U_1 \rangle$	$ U_2 \rangle$	$ U_3 \rangle$	$ U_4 \rangle$	$ U_5 \rangle$	$ U_6 \rangle$
$\langle U_0  $	-.00836	-.00896	-.0219	-.00889	-.00965	.00361	.00181
$\langle U_1  $	-.00896	-.0393	-.0281	-.0574	-.0103	-.0169	.00553
$\langle U_2  $	-.0219	-.0281	-.0948	-.0400	-.101	-.0938	-.0236
$\langle U_3  $	-.00889	-.0574	-.0400	-.165	-.0498	-.150	.00760
$\langle U_4  $	-.00965	-.0103	-.101	-.0498	-.245	-.0569	-.202
$\langle U_5  $	.00361	-.0169	-.0938	-.150	-.0569	-.332	-.0621
$\langle U_6  $	.00181	.00553	-.0236	-.00760	-.202	-.0621	-.424

Table 17:  $dV_{nm}$  terms for perturbation theory for various combinations of wave functions and difference between the harmonic oscillator and our calculated potential for gravitons in the L=4 state.



Wave Function	$ U_0\rangle$	$ U_1\rangle$	$ U_2\rangle$	$ U_3\rangle$	$ U_4\rangle$	$ U_5\rangle$	$ U_6\rangle$
$\langle U_0 $	-.00836	-.00896	-.0219	-.00889	-.00965	.00361	.00181
$\langle U_1 $	-.00896	-.0393	-.0281	-.0574	-.0103	-.0169	.00553
$\langle U_2 $	-.0219	-.0281	-.0948	-.0400	-.101	-.0938	-.0236
$\langle U_3 $	-.00889	-.0574	-.0400	-.165	-.0498	-.150	.00760
$\langle U_4 $	-.00965	-.0103	-.101	-.0498	-.245	-.0569	-.202
$\langle U_5 $	.00361	-.0169	-.0938	-.150	-.0569	-.332	-.0621
$\langle U_6 $	.00181	.00553	-.0236	-.00760	-.202	-.0621	-.424

Table 18:  $dV_{nm}$  terms for perturbation theory for various combinations of wave functions and difference between the harmonic oscillator and our calculated potential for photons in the L=1 state.

Wave Function	$ U_0\rangle$	$ U_1\rangle$	$ U_2\rangle$	$ U_3\rangle$	$ U_4\rangle$	$ U_5\rangle$	$ U_6\rangle$
$\langle U_0 $	-.00836	-.00896	-.0219	-.00889	-.00965	.00361	.00181
$\langle U_1 $	-.00896	-.0393	-.0281	-.0574	-.0103	-.0169	.00553
$\langle U_2 $	-.0219	-.0281	-.0948	-.0400	-.101	-.0938	-.0236
$\langle U_3 $	-.00889	-.0574	-.0400	-.165	-.0498	-.150	.00760
$\langle U_4 $	-.00965	-.0103	-.101	-.0498	-.245	-.0569	-.202
$\langle U_5 $	.00361	-.0169	-.0938	-.150	-.0569	-.332	-.0621
$\langle U_6 $	.00181	.00553	-.0236	-.00760	-.202	-.0621	-.424

Table 19:  $dV_{nm}$  terms for perturbation theory for various combinations of wave functions and difference between the harmonic oscillator and our calculated potential for photons in the L=2 state.

Wave Function	$ U_0\rangle$	$ U_1\rangle$	$ U_2\rangle$	$ U_3\rangle$	$ U_4\rangle$	$ U_5\rangle$	$ U_6\rangle$
$\langle U_0 $	-.00836	-.00896	-.0219	-.00889	-.00965	.00361	.00181
$\langle U_1 $	-.00896	-.0393	-.0281	-.0574	-.0103	-.0169	.00553
$\langle U_2 $	-.0219	-.0281	-.0948	-.0400	-.101	-.0938	-.0236
$\langle U_3 $	-.00889	-.0574	-.0400	-.165	-.0498	-.150	.00760
$\langle U_4 $	-.00965	-.0103	-.101	-.0498	-.245	-.0569	-.202
$\langle U_5 $	.00361	-.0169	-.0938	-.150	-.0569	-.332	-.0621
$\langle U_6 $	.00181	.00553	-.0236	-.00760	-.202	-.0621	-.424

Table 20:  $dV_{nm}$  terms for perturbation theory for various combinations of wave functions and difference between the harmonic oscillator and our calculated potential for photons in the L=3 state.

